ACS OMEGA

Open Access

This article is licensed under CC-BY-NC-ND 4.0

http://pubs.acs.org/journal/acsodf

Article

Quantum Chemical Investigation of the Interaction of Thalidomide Monomeric, Dimeric, Trimeric, and Tetrameric Forms with Guanine DNA Nucleotide Basis in DMSO and Water Solution: A Thermodynamic and NMR Spectroscopy Analysis

Haroldo C. Da Silva, Isabel S. Hernandes, and Wagner B. De Almeida*

Cite This: *ACS Omega* 2023, 8, 37521−37539

Read Online

ACCESS | Metrics & More | Article Recommendations | Supporting Information

ABSTRACT: Thalidomide (TLD) was used worldwide as a sedative, but it was revealed to cause teratogenicity when taken during early pregnancy. It has been stated that the (R) enantiomer of TLD has therapeutic effects, while the (S) form is teratogenic. Clinical studies, however, demonstrated the therapeutic efficacy of thalidomide in several intractable diseases, so TLD and its derivatives have played an important role in the development and therapy of anticancer drugs. Therefore, it is important to know the molecular mechanism of action of the TLD, although this is still not clear. In what molecular interactions are concerned, it is known that drug molecules can interact with DNA in different ways, for example, by intercalation between base pairs. Furthermore, the ability of the TLD to interact with DNA has been confirmed experimentally. In this work, we report a theoretical investigation of the interaction of the R and S enantiomers of TLD, in its monomeric, dimeric, trimeric, and tetrameric forms, with guanine (GUA) DNA nucleotide basis in solution using density functional theory (DFT). Our initial objective was to evaluate the interaction of TLD-R/S with GUA through thermodynamic and spectroscopic study in dimethyl sulfoxide (DMSO) solvent and an aqueous solution. Comparison of the experimental ^{1}H nuclear magnetic resonance (NMR) spectrum in DMSO-d_6 solution with calculated DFT-PCM-DMSO chemical shifts revealed that TLD can undergo molecular association in solution, and interaction of its dimeric form with a DNA base ($(TLD)_2$-GUA and $(TLD)_2$-2GUA, for example) through H-bond formation is likely to take place. Our results strongly indicated that we must consider the plausibility of the existence of TLD associations in solution when modeling the complexation of the TLD with biological targets. This is new information that may provide further insight into our understanding of drug binding to biological targets at the molecular level.

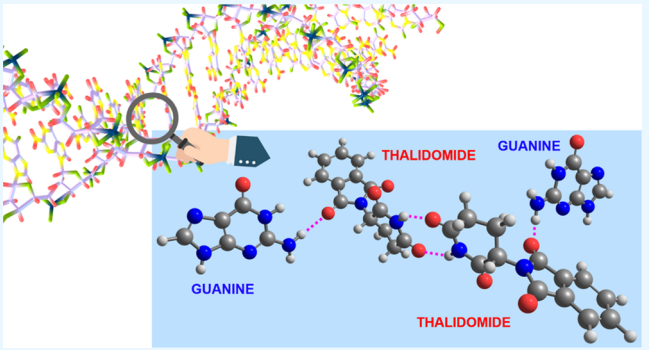

INTRODUCTION

Stereochemistry has been shown to play an important role in the metabolism of drugs and pharmacokinetics[1,2] because proteins, which are chiral by nature, are fundamental species in these biological processes. There are various reports in the literature about chemical compounds that can exist in two isomeric or enantiomeric forms that strongly influence biological activity. Cisplatin is very effective as an anticancer agent; however, the trans-isomer, transplatin, is clinically ineffective. Although both isomers target nuclear DNA, there is a large difference in the magnitude of their biological effects.[3] Two different enantiomers of the same compound may differ in their distribution, metabolism, excretion, and toxicity. One well-known example is thalidomide (TLD), which exists in two mirror-image forms: (R) and (S) enantiomers. While the (R) enantiomer has sedative effects, the (S) isomer is teratogenic.[4] However, it had been argued in other studies that both (R) and (S) enantiomers can be teratogenic, and due to fast racemization under biological conditions, experimental investigations using pure enantiomers may not be quite conclusive.[5,6]

TLD (see Scheme 1) was used worldwide as a sedative, but it was revealed to cause teratogenicity when taken during early pregnancy.[7−10] Clinical studies, however, demonstrated the therapeutic efficacy of thalidomide in several intractable diseases, with TLD and its derivatives playing an important role in anticancer drug development and therapy.[11,12] Although the molecular mechanism of action is still unclear, the discovery

Received: August 11, 2023
Accepted: September 13, 2023
Published: September 28, 2023

© 2023 The Authors. Published by American Chemical Society

Scheme 1. Structural Formulae of R-Thalidomide and S-Thalidomide (a) and Guanine (b) and Numbering Scheme[a]

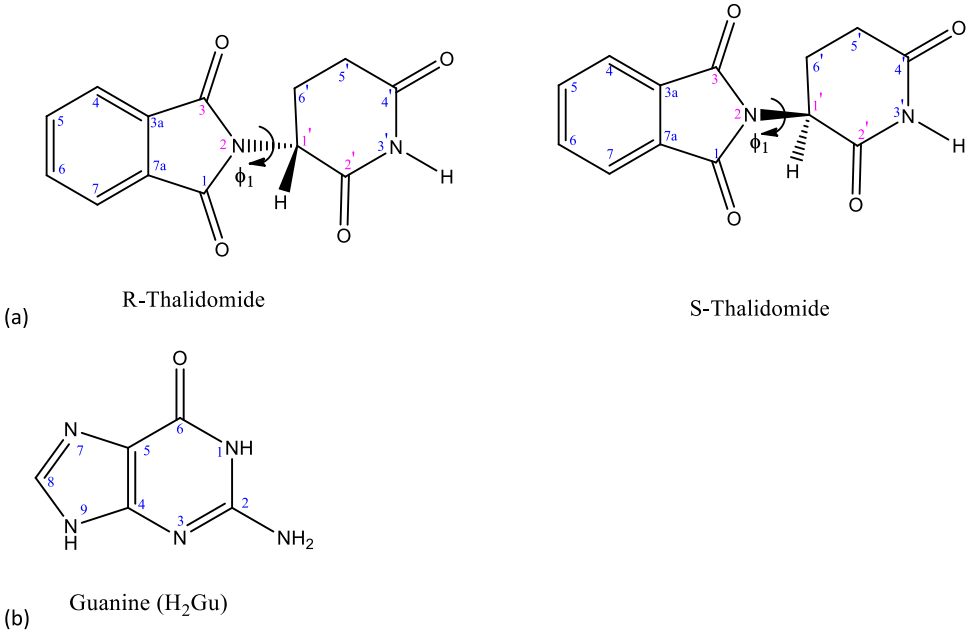

[a]The inter-ring torsion angle (ϕ_1) is also indicated.

of cereblon (CRBN) as a direct target of TLD some years ago[13] has made a great contribution to our understanding of its mechanism of action. CRBN is thought to act basically as a subunit of a ligand-dependent E3 ubiquitin ligase complex whose substrate recognition can be controlled by thalidomide or its related compounds.[14] The domain structure of human CRBN consists of a total of 441 amino acids; amino acids 79−316 are Lon substrate-binding domains, and amino acids 320−421 are IMiD drug-binding domains.[15] A review of the molecular mechanisms of the teratogenic effects of TLD was recently published.[16]

TLD can form asymmetric homochiral dimers in (S)-thalidomide, and (R)-thalidomide can form homochiral dimers and symmetric heterochiral dimers in the (RS)-thalidomide crystalline state and solution.[5,17] These results from ref 5 indicate that differences in physicochemical properties between enantiomeric and racemic forms of thalidomide originate from the difference in the structural stability between homochiral and heterochiral dimers. This raises the hypothesis that a TLD dimer may interact with DNA, which might explain the teratogenic effect. According to ref 5, these enantiomers form an equilibrium between themselves and between both homochiral and heterochiral dimers. It is believed that the more energetically favorable and stable heterochiral dimer of thalidomide is an active agent that possesses the structural features of paired nucleotides of double-stranded DNA. The existence of the R/S heterodimer was also used in ref 18, aiming at an understanding of the thalidomide chirality in biological processes. So far, no biological or theoretical study that could confirm the dimer stability in physiological conditions has been carried out.

Drug molecules can interact with DNA in different ways, for example, by intercalation between base pairs, covalent attachments to the double helix, etc. The intercalation of TLD with DNA has been addressed some time ago,[19,20] with the plausibility of the interaction between TLD and DNA being confirmed using electrochemical and atomic force microscopy methods.[21]

A theoretical investigation of the interaction of the (S)-TLD enantiomer with DNA nucleobases was reported recently,[22] where extensive density functional theory (DFT)[23] calculations (in the vacuum) considering adenine, guanine, cytosine, and thymine were carried out, with the analysis of infrared spectra also being performed. Calculated binding and interaction energies indicated that the (S)-TLD-Guanine complex exhibits a strong interaction in the gas phase. There are other previous theoretical reports on TLD referring to the molecular structure and spectroscopic analysis[24−34] but without focus on the thermodynamic and NMR (nuclear magnetic resonance) analysis in solution, which is the objective of this theoretical study.

Therefore, considering these available results about TLD, we realized that a more complete theoretical investigation of the interaction of TLD R/S enantiomers in its monomeric and molecular association forms (dimer, trimer, and tetramer) with DNA bases in solution is certainly of relevance. Solvent effects must be considered to more closely model the experimental environment of the TLD interacting with biological targets. In this work, we used the DFT methodology[23] to perform a thermodynamic and NMR analysis of the interaction of guanine with (S) and (R)-TLD and corresponding molecular associations (**RS**, **SS**, **RR**, R-**RS**, **RS**-S, R-**SS**, **SS**-S, **RR**-**RS**, **RR**-**SS**, **RS**-**SS**, **SS**-**SS**), encompassing homochiral (**RR** and **SS**) and heterochiral (**RS**) dimers. The bold letters indicate the type of dimer structures used to build the TLD trimer and tetramer. Solvent effects (DMSO and water) were taken into account by employing the PCM (polarizable continuum model)[35] and also including explicit solvent molecules (representing the first solvation shell) in the DFT-PCM geometry optimization procedure. By accurately simulating the TLD-Guanine interaction in solution, we can assess if there is a preference for the R or S forms of TLD for interacting with the DNA base, which may be somehow related to the biological activity.

https://doi.org/10.1021/acsomega.3c05922
ACS Omega 2023, 8, 37521−37539

COMPUTATIONAL DETAILS

The two enantiomeric R and S structures of TLD were first optimized in vacuum at the DFT[23] level with the ωB97x-D functional,[36] which carries a dispersion correction and has been found very satisfactory for the description of thermochemistry and noncovalent interactions, using the 6-31G(d,p) basis set,[37] followed by harmonic frequency calculations to characterize the optimized structures as true minima (no imaginary frequency) on the potential energy surface (PES). Then, the geometries were reoptimized taking solvent effects (DMSO and water) into account using the polarizable continuum model (PCM).[35] In the next step, dimer, trimer, and tetramer formation was considered using all R/S TLD monomer combinations, followed by DFT geometry optimization of TLD molecular association structures.

To improve the solvent description, "*n*" explicit DMSO solvent molecules were included in the DFT geometry optimization procedure: $n = 0$ (PCM-Only), $n = 1$, $n = 2$, $n = 3$, $n = 4$, $n = 6$, $n = 8$ and $n = 20$ (our best model encompassing short- and long-range solute−solvent interactions). We have shown that such a procedure worked very fine for the prediction of NMR chemical shifts of N−H protons in nitrogenated compounds[38] and O−H protons in isoflavones[39] and chloroquine/hydroxychloroquine,[40] in chloroform solutions. The PCM-nDMSO optimized geometries were used in DFT-PCM NMR calculations of shielding constants (σ) with chemical shifts (δ) determined on a δ scale relative to tetramethylsilane (TMS) internal reference using the gauge-independent atomic orbital (GIAO) method[41] and the hybrid B3LYP functional.[42,43]

Initial (S) TLD-Guanine complex structures, having strong interactions in the gas phase among the four DNA bases, were taken from ref 22. That was the reason for choosing guanine instead of other nuclear bases, which we believe is representative of the interactions with nuclear bases (and makes the work computationally viable). Three low-energy (S) TLD-Guanine complexes, named here as **I**, **II**, and **III**, were considered representative on an energetic basis. Then, we inverted the chiral center and generated the corresponding (R) TLD-Guanine complexes. We used these (R/S) complex structures as inputs for ωB97x-D/6-31G(d,p)-PCM geometry optimization. Finally, the lowest energy TLD-Guanine complexation mode (Complex **II**) was used as the model spatial orientation in the geometry optimization for the guanine complexes with TLD dimer, trimer, and tetramer structures.

All quantum chemical calculations were performed with the Gaussian 09 package.[44]

RESULTS AND DISCUSSION

Free Thalidomide in Solution. Inter-ring torsion angle ϕ_1 (deg) [C2′, C1′, N2, C3] and relative energies (ΔE_{rel} in kcal mol^{-1}) for free TLD R/S DFT-optimized structures in the vacuum, using the PCM solvent model (PCM-Only) and including "*n*" explicit solvent molecules (PCM-*n*DMSO) are given in Table 1 with selected ωB97x-D/6-31G(d,p)-PCM optimized structures shown in Figure 1. Relative energy values (relative Gibbs free energies (ΔG_{rel}) are given in parentheses) range approximately from −2 to +2 kcal mol^{-1}, indicating that there is no remarkable preference for the R or S structure. Torsion angle ϕ_1 has a small change (1.2−2.7°) comparing PCM and vacuum values, with larger changes (up to 5.2°) observed for PCM-*n*DMSO results.

Table 1. ωB97x-D/6-31G(d,p)-PCM-*n*DMSO Relative Energies and Torsion Angle for TLD Free

	ΔE_{rel}[a,b] (kcal mol^{-1})		ϕ_1 (deg) [C2′, C1′, N2, C3]	
Free TLD (monomer)	R	S	R	S
PCM-vacuum	0.0	−1.9 (−1.7)[c]	−44.8	60.7
PCM-only	0.0	−2.0 (−2.2)[c]	−46.0	58.0
PCM-1DMSO	0.0	−1.9 (−3.0)[c]	−43.8	60.9
PCM-2DMSO	0.0	1.9 (1.1)[c]	−37.8	58.7
PCM-3DMSO	0.0	0.1 (−1.2.)[c]	−47.9	59.9
PCM-4DMSO	0.0	0.5 (−2.1)[c]	−44.3	61.1
PCM-6DMSO	0.0	0.7	−50.0	54.6
PCM-8DMSO	0.0	1.8	−48.1	53.8
PCM-20DMSO	0.0	1.6	−44.1	56.1

[a]Relative energy is evaluated concerning the R (monomer) structure. [b]The sign of ΔE_{rel} can be positive or negative depending on the initial guess solvated structure used in the DFT geometry optimization procedure. [c]ΔG_{rel} values are given in parentheses.

Figure 1 shows three PCM-*n*DMSO ($n = 1$, $n = 8$, and $n = 20$) explicitly solvated optimized structures, with solute−solvent distances indicated by traced lines. There is a short H-bond (1.7−1.8 Å) formed between the O═S group of DMSO solvent and the N−H group of TLD present in all solvated structures. The O···S═O solute−solvent distances are in the range of 2.9−3.8 Å. From the results reported in Table 1 and Figure 1, it can be seen that the conformation of the TLD is practically undisturbed due to the interaction with DMSO solvent molecules.

Experimental ^{1}H NMR chemical shift data (in DMSO-d_6) reported for TLD in refs 45,46 are shown in Figure 2 along with the corresponding theoretical spectra (B3LYP/6-31G(d,p)-PCM-DMSO) for the selected TLD optimized structures. It can be promptly seen that the use of the PCM model without including explicit DMSO solvent molecules is not adequate to reproduce the remarkable **N−H** NMR signal experimentally observed at 11.0 ppm. This shows that a strong solute−solvent **N−H**···O═S H-bond is required to obtain a good match with experimental NMR data. For all R and S enantiomer-solvated structures, a similarly good agreement with the experimental NMR profile is achieved. The NMR spectrum cannot be used to differentiate between the two enantiomers in the DMSO solution; in fact, the two spectra are very similar, although the chemical environment around the CH_n and N−H protons may look distinct for enantiomers R and S (see Figure 2). A comparison between PCM-Only (without explicit solvent molecules) and PCM-*n*DMSO ^{1}H NMR spectra with the experimental NMR pattern reveals that only the **N−H** group must be near a DMSO molecule to reach a good agreement with the experimental NMR profile. Therefore, the CH_n protons must not be very close to DMSO solvent molecules (the distance should be larger than approximately 3 Å); otherwise, a large deviation between calculated and experimental chemical shifts is observed for CH_n protons. All structures shown in Figure 2 yielded good agreement with the experimental spectrum regarding the ^{1}H NMR profile for CH_n protons. It is opportune to mention that the PES for the solvated molecular structure (TLD-PCM-*n*DMSO) has many local minima, and the final optimized geometry structure may not necessarily well reproduce the experimental CH_n chemical shifts due to the proximity with DMSO solvent molecules during the course of the geometry optimization procedure. Nevertheless, we can pick up a local minimum that leads to a good match with the whole

https://doi.org/10.1021/acsomega.3c05922
ACS Omega 2023, 8, 37521−37539

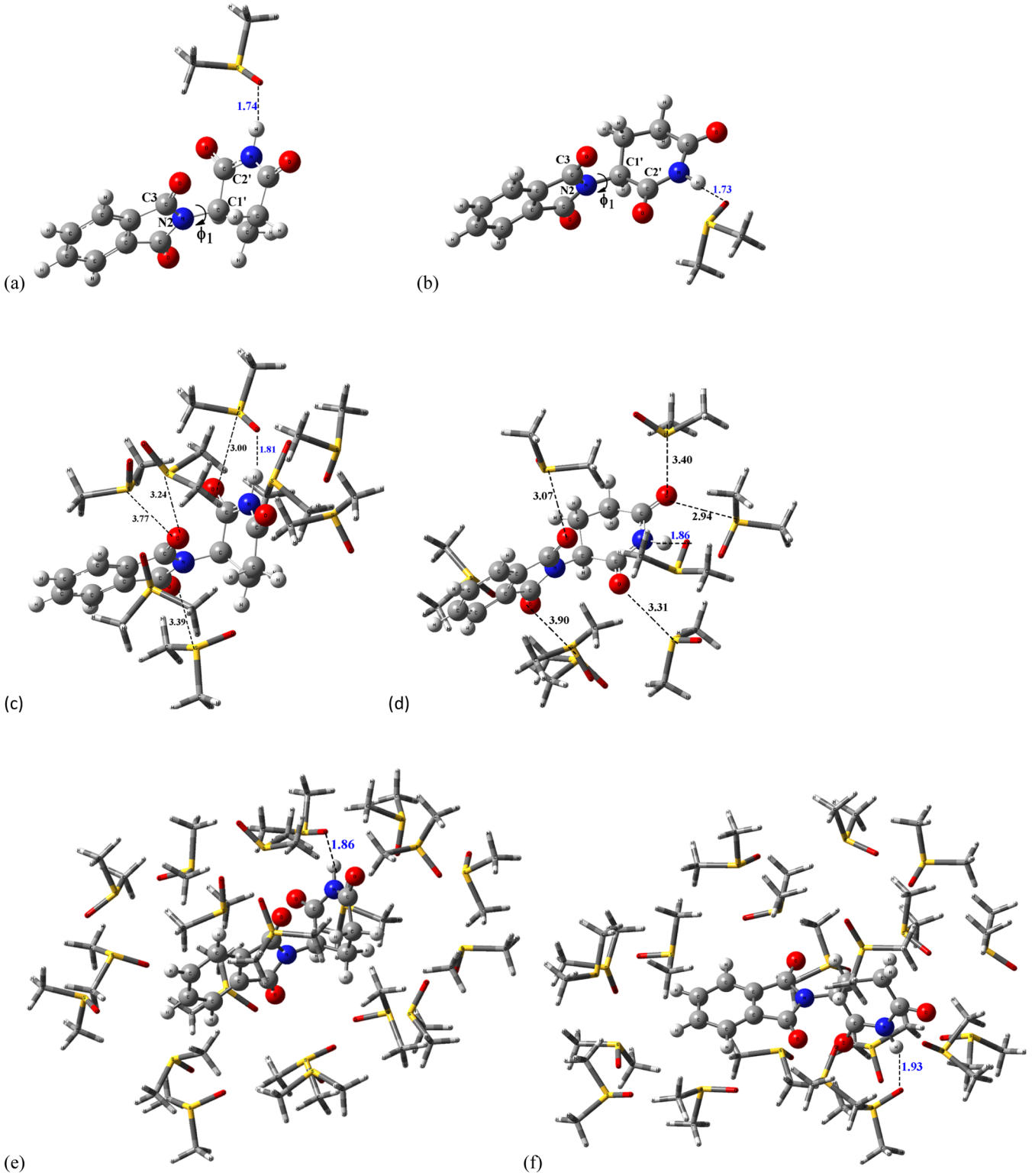

Figure 1. ωB97x-D/6-31G(d,p)-PCM-DMSO optimized TLD monomer structures. (a) **R-1DMSO**, (b) **S-1DMSO**, (c) **R-8DMSO**, (d) **S-8DMSO**, (e) **R-20DMSO**, and (f) **S-20DMSO**.

^{1}H NMR spectrum (CH_n and N−H protons). Statistical index values (MAE) are also quoted in Figure 2, which support the ^{1}H NMR data.

The formation of dimeric structures of TLD has been considered in previous experimental works[5,17,47], which motivates us to investigate the plausibility of the occurrence of molecular associations involving TLD (dimer, trimer, and tetramer). Following experimental findings in the solid state, in this work, we explored various possibilities for the formation of R/S dimers, which led to eight relevant DFT-PCM optimized structures shown in Figure 3 with relative energies given in Figure 4. We took the mode of interaction of the lowest energy structure **3** (Figure 3c) as the most probable to exist and use it as a model input for optimizing the geometries of all combinations

https://doi.org/10.1021/acsomega.3c05922
ACS Omega 2023, 8, 37521−37539

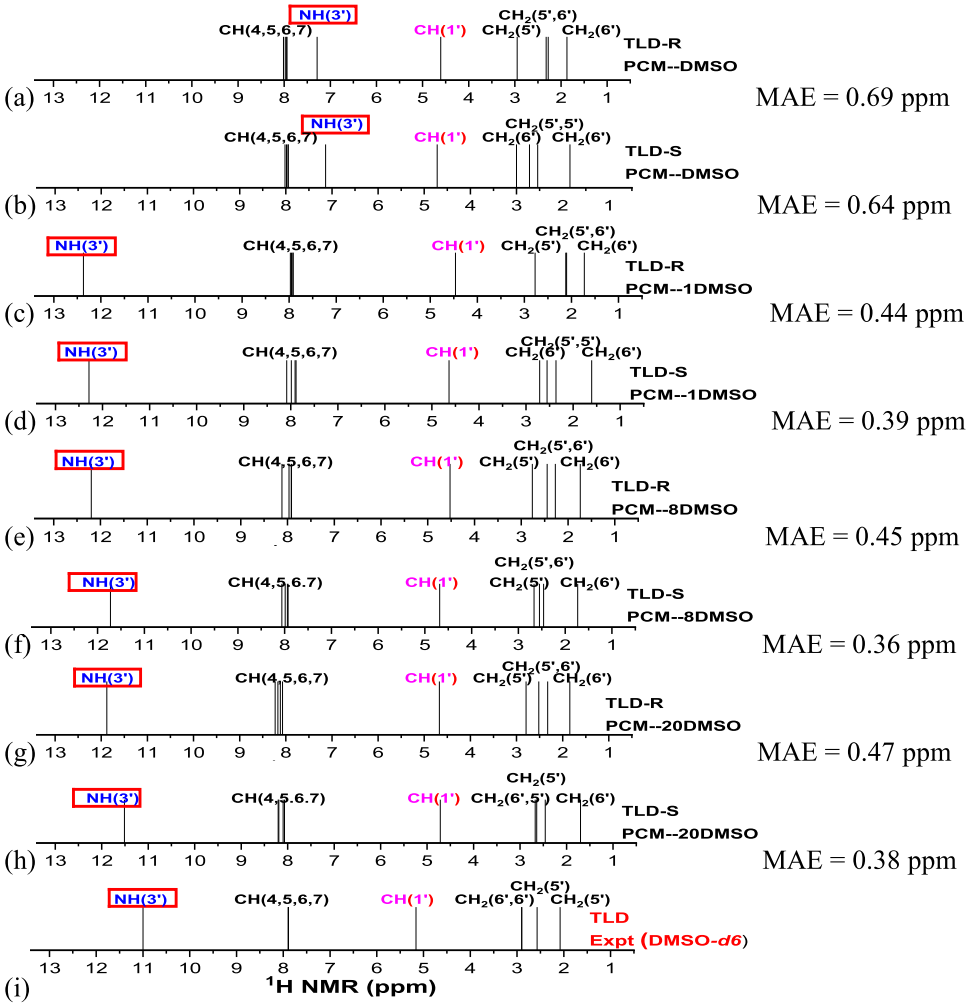

Figure 2. (a–h) B3LYP/6-31G(d,p)-PCM-DMSO and (i) experimental (DMSO-d_6) ^{1}H NMR spectra for TLD structures.

of the two R/S enantiomers: **RS**, **SS**, and **RR** dimers. Calculated relative energies (ΔE_{rel}) and energies of dimer, trimer, and tetramer formation ($\Delta E_{formation}$) are given in Table 2. Enthalpy of formation is given in parentheses, being almost the same as $\Delta E_{formation}$, but the Gibbs free energies of formation, also quoted in parentheses, are slightly positive. Although the RR dimer is plausible to exist based on the energy of formation values, it has not been considered in previous experimental reports. In the next step, the **R** and **S** combinations were considered for creating trimer (R-**RS**, **RS**-S, R-**SS**, **SS**-S) and tetramer (**RR-RS**, **RR-SS**, **RS-SS**, **SS-SS**) structures, and it was verified that the **RS**-S and **RS-SS** structures have the best energy of formation value for the trimer and tetramer, respectively, which is larger than the dimer value. The structures were reoptimized including 6, 9, and 12 explicit DMSO solvent molecules, respectively, for the dimer, trimer, and tetramer. All structures have favorable energy of formation values.

Basis set superposition error (BSSE) was evaluated for dimer structures using the counterpoise method.[48−50] BSSE corrected energies evaluated using the 6-31G(d,p)[37] and 6-311+G-(2d,p)[37] basis sets are given in Table 3. As expected, the BSSE correction for the small basis set is larger (around 3 kcal mol^{-1} (19%)) than that for the triple-ζ quality basis set (around 1 kcal mol^{-1} (5%)). The good dimer BSSE corrected stabilization (>11 kcal mo1^{-1}) gives support to the existence of molecular associations in solution.

Table 4 reports DFT-PCM-PCM optimized torsion angle ϕ_1 (deg) values for the TLD dimer, trimer, and tetramer. The effect of including explicit DMSO solvent molecules in the geometry optimization can be promptly seen, with variations in the range 2−8° being observed. There is no noticeable conformation change due to the interaction of TLD with explicit solvent molecules (and the use of the PCM solvent model).

Experimental (in DMSO-d_6) and B3LYP/6-31G(d,p)-PCM-DMSO ^{1}H NMR spectra for TLD dimer, trimer, and tetramer structures, calculated using the PCM model (PCM-Only) and including explicit DMSO solvent molecules (PCM-nDMSO) are shown in Figure 5. It can be seen that both PCM-Only and PCM-nDMSO spectra show reasonable agreement with the experimental profile, which is also reflected in the MAE values also quoted in Figure 5. The remarkable value of the experimental **N−H** chemical shift (11.0 ppm) is correctly reproduced by all TLD associations, where it is possible to observe that the analysis of NMR data provides support for the formation of TLD dimers, trimers, and tetramers in DMSO solution. DFT-optimized solvated structures (ωB97x-D/6-31G(d,p)-PCM level) of TLD dimers are shown in Figure 6. Trimer and tetramer structures are visualized in Figure 7. Intradimer H-bonds are indicated in blue traced lines and solute−solvent H-bonds in black traced lines. There is a strong N−H···O=C H-bond (short distance) involving two TLD monomers, which correlates well with experimental **N−H** ^{1}H

https://doi.org/10.1021/acsomega.3c05922
ACS Omega 2023, 8, 37521−37539

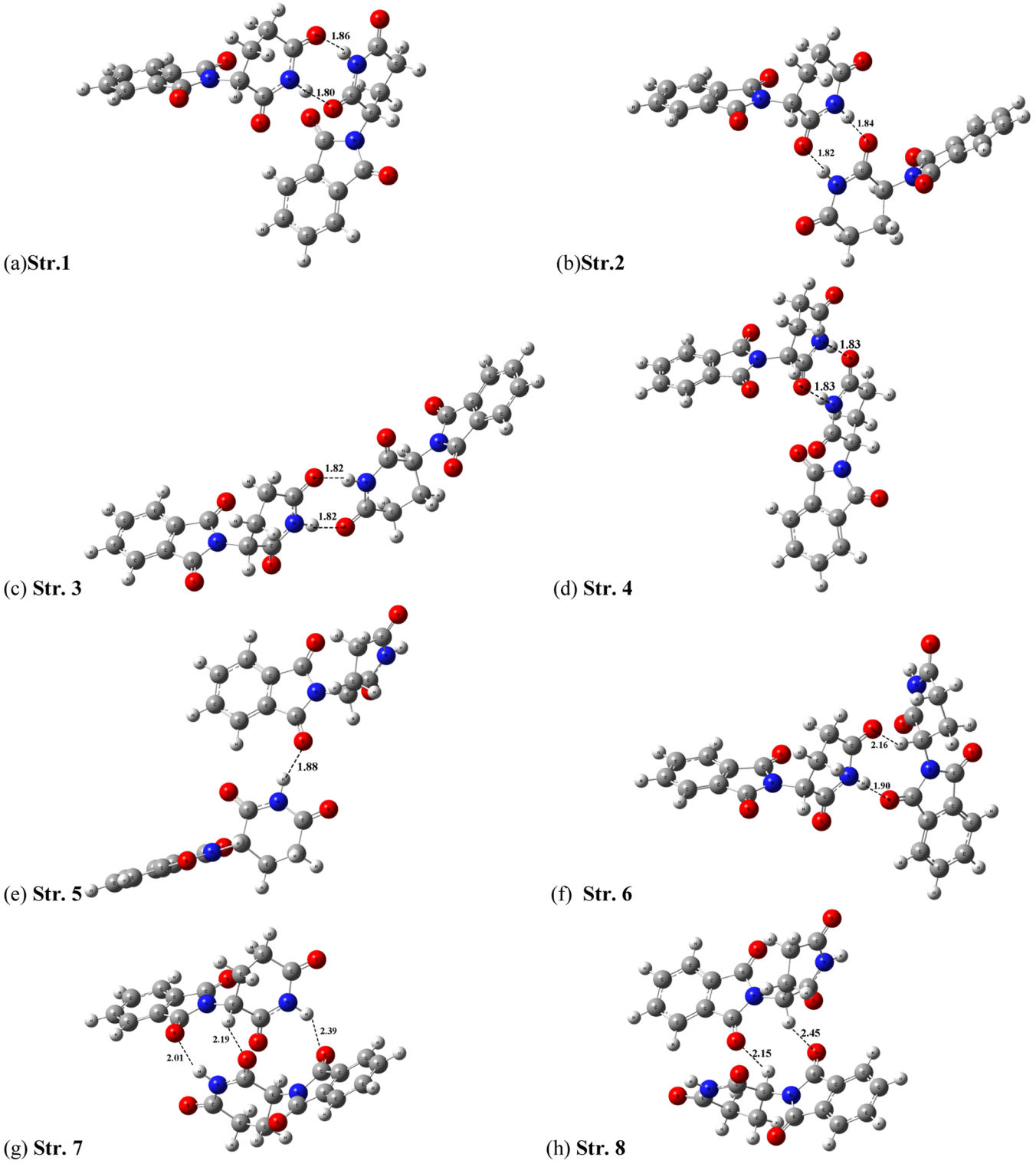

Figure 3. Structures (a) **1**, (b) **2**, (c) **3**, (d) **4**, (e) **5**, (f) **6**, (g) **7**, and (h) **8**: relevant TLD RS dimers ωB97x-D/6-31G(d,p)-PCM-DMSO optimized structures.

NMR data in DMSO-d_6. These model-solvated structures are a good representation of the main solute−solvent interaction.

Experimental evidence of the formation of the TLD dimer in solution would be available from the analysis of ^{1}H NMR data in $CDCl_3$. The solute−solvent interaction is much weaker when $CHCl_3$ is used as a solvent than DMSO, in DFT-PCM optimized structures including explicit solvent molecules, not contributing to enhance the **N−H** NMR signal. Since the **N−H** group can strongly interact with polar solvents, the effect on the respective ^{1}H NMR chemical shift value is pronounced for the DMSO solvent. Figure 8 shows a comparison of DFT-calculated ^{1}H NMR spectra for PCM-Only and PCM-6$CHCl_3$ optimized TLD R and S monomer structures where it can be seen that the presence of explicit $CHCl_3$ solvent molecules does not cause a significant increase in the **N−H** chemical shift value because of a

https://doi.org/10.1021/acsomega.3c05922
ACS Omega 2023, 8, 37521−37539

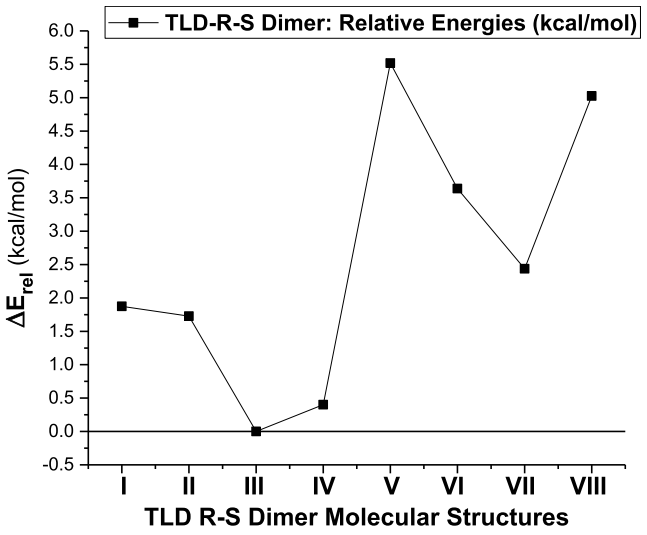

Figure 4. ωB97x-D/6-31G(d,p)-PCM-DMSO relative energies (kcal mol^{-1}) for TLD dimers (R/S configuration).

weaker interaction with the chloroform solvent molecules compared to DMSO.

According to our theoretical results, the strong interaction between the **N−H** group and DMSO solvent, which substantially enlarge the respective ^{1}H NMR chemical shift, masks the observation of the TLD dimer, which also cause a remarkable increase in the **N−H** chemical shift. As it becomes impossible to avoid the influence of the proton density on the signal strength, it is estimated that some signals are masked by differences in proton densities. We expected that the ^{1}H NMR data for TLD in $CDCl_3$ would be like DMSO solution, as happened with acetic acid (see Figure 9) where a similar O−H chemical shift is observed for acetic acid in both $CDCl_3$[51,52] and DMSO-d_6.[52,53] This is a well-known example where it could be established that the large O−H chemical shift value observed in $CDCl_3$ solution is unquestionably due to the acetic acid dimer formation, where two strong O−H···O═C H-bonds are formed.[54] Unfortunately, there is no NMR data for TLD in $CDCl_3$ due to the very poor solubility in chloroform to definitively confirm the TLD dimer formation as happened with acetic acid dimer.

It is opportune to mention that the role played by explicit solvent effects on the molecular conformation and chemical reaction viability and selectivity was discussed in detail in ref 55. A known chemical reaction whose selectivity depends on solvents with a low dielectric constant and small dipole moment, where the implicit solvation models do not account for the

Table 3. ωB97x-D/6-31G(d,p) BSSE Corrected Energy of TLD Dimer Formation (in Units of kcal mol^{-1})

	$\Delta E_{formation}$ BSSE corrected		
TLD dimer	**RS**	**SS**	**RR**
vacuum-OPT-geometry	−11.6	−15.1	−11.4
6-31G(d,p)	(2.7)[a]	(3.5)[a]	(2.7)[a]
6-311+G(2d,p)	−11.1	−14.4	−10.9
	(0.6)[a]	(0.7)[a]	(0.6)[a]

[a]BSSE correction is given in parentheses.

Table 4. ωB97x-D/6-31G(d,p)-PCM-DMSO Torsion Angle ϕ_1 (deg) for TLD Dimer, Trimer, and Tetramer

	ϕ_1 (deg) [C2′, C1′, N2, C3]			
	Mon-1	Mon-2	Mon-3	Mon-4
dimer **R-S**-vacuum-OPT-Geom.	−45.3	60.6		
dimer **R-S**-PCM-only	−45.1	60.5		
dimer **R-S**-PCM-6DMSO	−48.9	58.4		
dimer **S-S**-vacuum-OPT-Geom.	59.9	61.1		
dimer **S-S**-PCM-Only	59.1	61.8		
dimer **S-S**-PCM-6DMSO	67.1	61.8		
dimer **R-R**-vacuum-OPT-Geom.	−44.1	−43.9		
dimer **R-R**-PCM-only	−43.0	−43.8		
dimer **R-R**-PCM-6DMSO	−39.5	−36.3		
trimer **RS-S**-vacuum-OPT-Geom.	−44.2	61.6	58.2	
trimer **RS-S**-PCM-only	−45.1	60.5	58.0	
trimer **RS-S**-PCM-9DMSO	−50.2	65.3	55.8	
tetramer **RS-SS**-vacuum-OPT-Geom.	−44.4	60.4	58.8	58.6
tetramer **RS-SS**-PCM-only	−44.9	62.4	57.3	57.6
tetramer **RS-SS**-PCM-12DMSO	−50.5	61.1	57.0	55.3

Table 2. ωB97x-D/6-31G(d,p)-PCM-DMSO Relative Energies (ΔE_{rel}) and Energies of Formation ($\Delta E_{formation}$) for the TLD Dimer, Trimer, and Tetramer (in Units of kcal mol^{-1})[e]

	ΔE_{rel}[a]				$\Delta E_{formation}$[b]			
TLD dimer	**RS**	**SS**	**RR**		**RS**	**SS**	**RR**	
PCM-DMSO-OPT-geometry	0.0	−2.3	1.9		−11.8 (−10.1)[c] (2.1)[d]	−11.7 (−10.1)[c] (2.2)[d]	−11.5 (−9.7)[c] (3.0)[d]	
PCM-4DMSO-OPT-geometry	0.0	7.3	7.7		−5.5	3.8	0.25	
PCM-6DMSO-OPT-geometry	0.0	1.9	7.5		−7.9[d]	−4.1[d]	−2.4[d]	
TLD trimer	**R-RS**	**RS-S**	**R-SS**	**SS-S**	**R-RS**	**RS-S**	**R-SS**	**SS-S**
PCM-DMSO-OPT-geometry	0.0	−3.5	−1.4	−3.6	−14.5	−16.0	−13.8	−14.1
PCM-6DMSO-OPT-geometry					9.6	−15.3[e]		
PCM-9DMSO-OPT-geometry					−11.2	−11.5[e]		
TLD tetramer	**RR-RS**	**RR-SS**	**RS-SS**	**SS-SS**	**RR-RS**	**RR-SS**	**RS-SS**	**SS-SS**
PCM-DMSO-OPT-geometry	0.0	−4.3	−8.8	−8.14	−14.6	−16.9	−19.5	−16.9
PCM-8DMSO-OPT-geometry						−25.6	−12.2[f]	
PCM-12DMSO-OPT-geometry						37.4	−17.5[f]	

[a]Relative energy is evaluated concerning **RS** (dimer), **R-RS** (trimer), and **RR-RS** (tetramer) structures. [b]Energy of formation is defined as the difference between total energies of dimer, trimer, and tetramer and the sum of monomer energies. [c]$\Delta H_{formation}$ value. $\Delta G_{formation}$ is given in parentheses.. [d]Energy of solvated dimer formation: $\Delta E_{formation} = E_{tot}$ (Dimer-6DMSO) − (E(TLD-R)) + (E(TLD-S)) + 6E(DMSO). [e]Energy of solvated trimer formation: $\Delta E_{formation} = E_{tot}$ (Trimer-9DMSO) − (E(TLD-R)) + 2(E(TLD-S)) + 9E(DMSO). [f]Energy of solvated tetramer formation: $\Delta E_{formation} = E_{tot}$ (Tetramer-12DMSO) − (E(TLD-R)) + 3(E(TLD-S)) + 12E(DMSO).

https://doi.org/10.1021/acsomega.3c05922
ACS Omega 2023, 8, 37521−37539

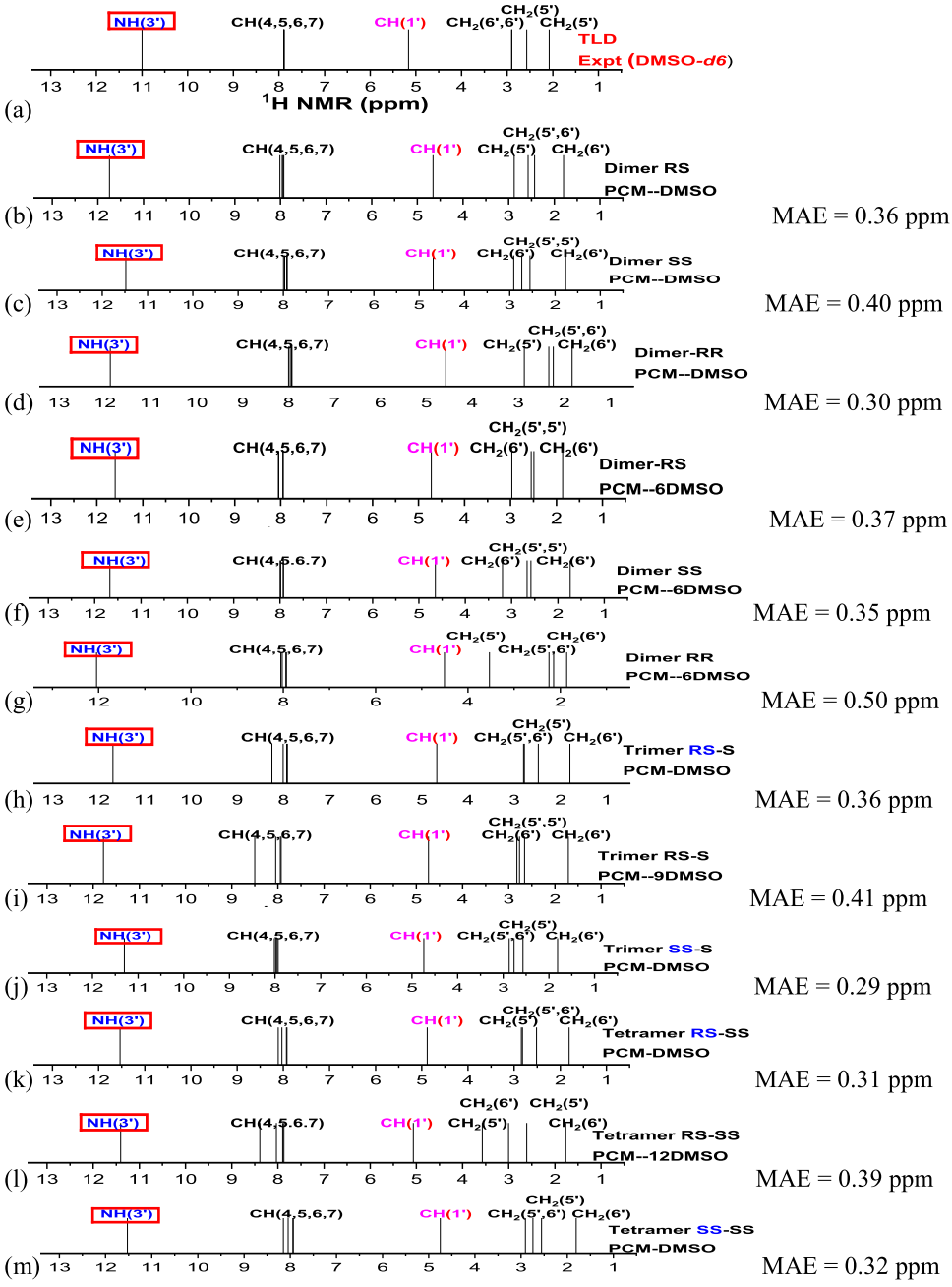

Figure 5. (a) Experimental (DMSO-d_6) and (b−m) B3LYP/6-31G(d,p)-PCM-DMSO//ω97x-D/6-31G(d,p)-PCM-DMSO ^{1}H NMR spectra for TLD structures.

Table 5. ωB97x-D/6-31G(d,p)-DMSO Relative Energies for TLD-Guanine Complexes (ΔE_{rel}, ΔH_{rel}, ΔG_{rel}, in kcal mol^{-1})

PCM-DMSO-OPT-geometry	relative energies (kcal mol^{-1})					
TLD monomer	R	S	R	S	R	S
TLD-Guanine complex	Cpx-I		Cpx-II		Cpx-III	
ΔE_{rel}	2.5	1.0	1.9	0.0	6.2	2.8
ΔH_{rel}	2.6	1.0	2.1	0.0	6.6	2.9
ΔG_{rel}	2.7	0.5	2.0	0.0	6.3	2.0

difference in the product ratios, was used as an example. The subject of how many solvent molecules should be added and where they should be placed to understand the role of the explicit solvent in reaction selectivity was properly addressed.

Guanine-Thalidomide Complexes in Solution. Three representative modes of interaction between guanine and TLD (R and S forms) were considered, enumerated Complexes **I**, **II**, and **III** (R and S enantiomers). The ωB97x-D/6-31G(d,p)-PCM-DMSO optimized structures are shown in Figure 10. The lowest energy Complex II (see Table 5) was used as input to build dimer (Figure 11), trimer, and tetramer (Figure 12) Guanine-TLD complex structures. Relative energy values (ωB97x-D/6-31G(d,p)-PCM-DMSO) for TLD-Guanine complexes (ΔE_{rel}, ΔH_{rel}, and ΔG_{rel}, in units of kcal mol^{-1}) are given in Table 5. Essentially, the same ΔE_{rel} energy trend is predicted by calculations including thermal correction (p = 1 atm, T = 298.15 K), evaluated using standard statistical thermodynamic formulas.[56]

https://doi.org/10.1021/acsomega.3c05922
ACS Omega 2023, 8, 37521−37539

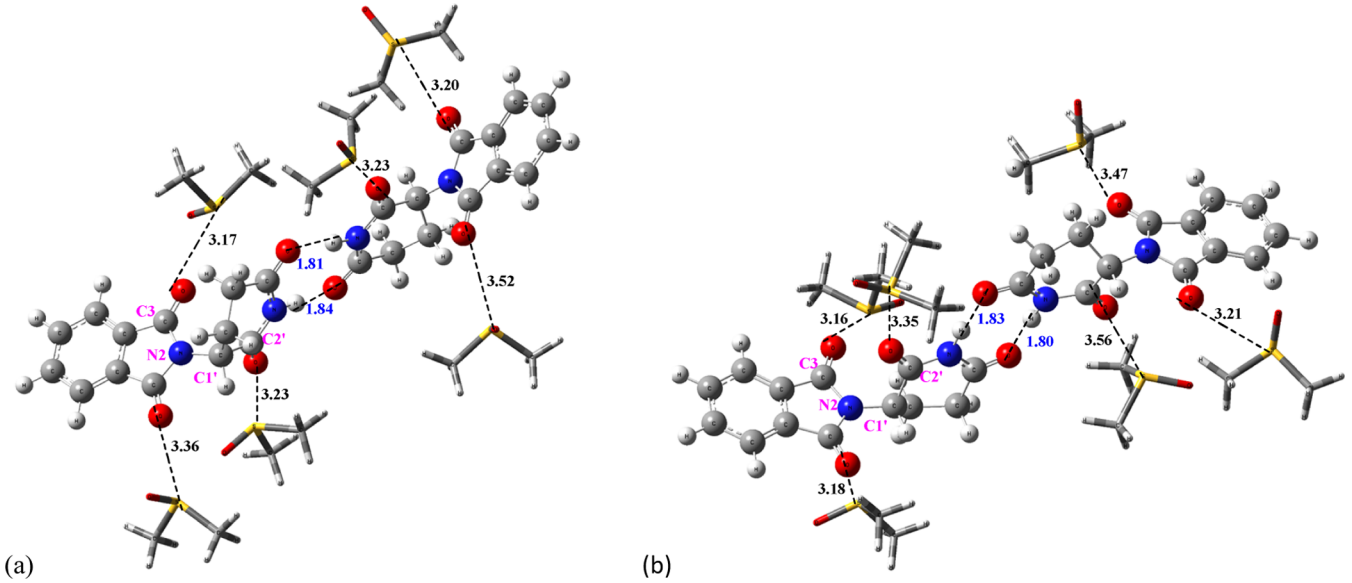

Figure 6. ωB97x-D/6-31G(d,p)-PCM optimized TLD dimer structures. (a) **RS-Dimer-PCM-6DMSO** and (b) **SS-Dimer-PCM-6DMSO**.

Table 6. ωB97x-D/6-31G(d,p) Energy of Formation (in Units of kcal mol^{-1}) for TLD-Guanine Complexes[a]

vacuum-OPT-geometry	$\Delta E_{formation}$[b]					
TLD monomer	**R**	**S**	**R**	**S**	**R**	**S**
TLD-Guanine complex	Cpx-I		Cpx-II		Cpx-III	
6-31G(d,p)	−19.3 (−16.4)[c]	−19.5 (−16.6)[c]	−19.8 (−16.8)[c]	−19.6 (−16.6)[c]	−17.8 (−14.4)[c]	−18.9 (−15.8)[c]
6-311+G(2d,p)	−16.5 (−15.9)[d]	−16.7 (−16.1)[d]	−17.0 (−16.5)[d]	−16.8 (−16.3)[d]	−15.3 (−14.5)[d]	−16.4 (−15.8)[d]
Aug-cc-pVDZ			−17.5 (−16.5)[d]	−17.3 (−16.3)[d]		
Aug-cc-pVTZ			−16.9 (−16.5)[d]	−16.7 (−16.3)[d]		
TLD dimer	**RS**	**SS**	**RS**	**SS**	**RS**	**SS**
TLD-dimer-Gua complex	Cpx-IV		Cpx-V		Cpx-VI	
6-31G(d,p)	−6.3	−7.7	−11.3 (−8.7)[c]	−8.1 (−6.4)[c]	−6.1	−5.4
6-311+G(2d,p)			−9.4 (−8.8)[d]	−6.8 (−6.4)[d]		
TLD trimer	**RS**-S	**RS**-S				
TLD-trimer-Gua complex	Cpx-VII	Cpx-VIII				
6-31G(d,p)	−6.8	−11.2 (−9.0)[c]				
6-311+G(2d,p)		−9.6 (−9.0)[d]				
TLD tetramer	**RS-SS**	**RS-SS**				
TLD-tetramer-Gua complex	Cpx-IX	Cpx-X				
6-31G(d,p)	−9.9	**−14.5** (−12.3)[c]				
6-311+G(2d,p)		**−9.6** (−8.9)[d]				

[a]BSSE corrected energy values are given in parentheses. Single-point energy values with larger basis sets are also reported. [b]Energy of formation is defined as the difference between the total energy of GUA-TLD complex and the sum of total energies of guanine and TLD monomer, dimer, trimer, and tetramer. [c]ωB97x-D/6-31G(d,p) BSSE corrected energies of formation value. [d]BSSE corrected energies of formation value (single-point calculation).

The basis set superposition error (BSSE) was evaluated using the counterpoise method.[48−50] Energies of complex formation (in units of kcal mol^{-1}) for structures optimized in the vacuum are given in Table 6 since BSSE correction calculations using an implicit solvent (PCM) cannot be performed within the Gaussian package. BSSE corrected energies evaluated using four basis sets, 6-31G(d,p),[37] 6-311+G(2d,p),[37] aug-cc-pVDZ,[57] and aug-cc-pVTZ,[57] are reported in Table 6 in

https://doi.org/10.1021/acsomega.3c05922
ACS Omega 2023, 8, 37521−37539

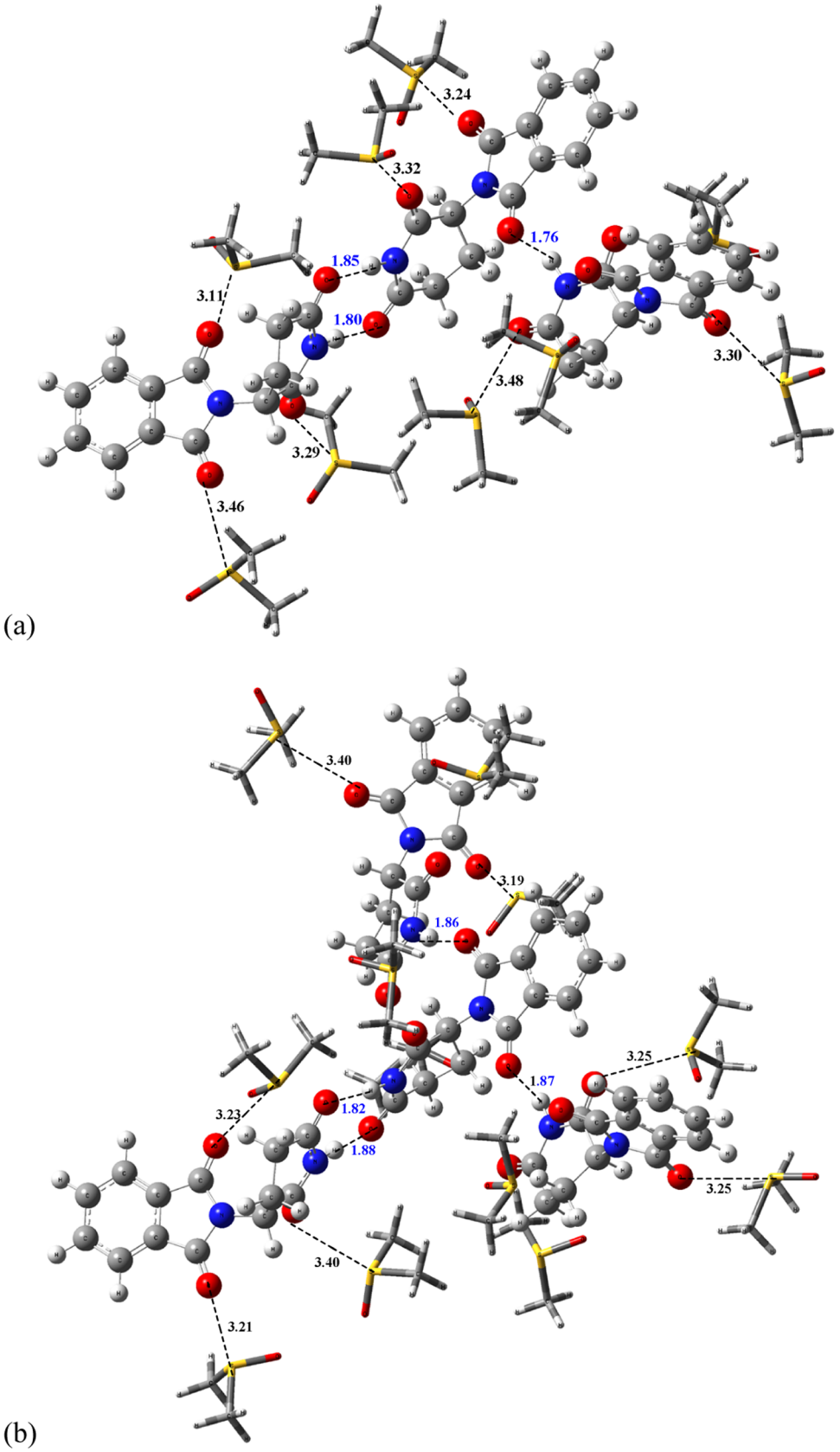

Figure 7. ωB97x-D/6-31G(d,p)-PCM-DMSO optimized TLD trimer and tetramer structures. (a) Trimer **RS**-S **PCM-9DMSO** and (b) Tetramer **RS-SS PCM-12DMSO**.

parentheses. It can be seen that the BSSE correction is relatively moderate using the smallest 6-31G(d,p) basis set, with essentially the same energy profile being predicted in all calculations. The largest BSSE correction for the 6-31G(d,p)

https://doi.org/10.1021/acsomega.3c05922
ACS Omega 2023, 8, 37521−37539

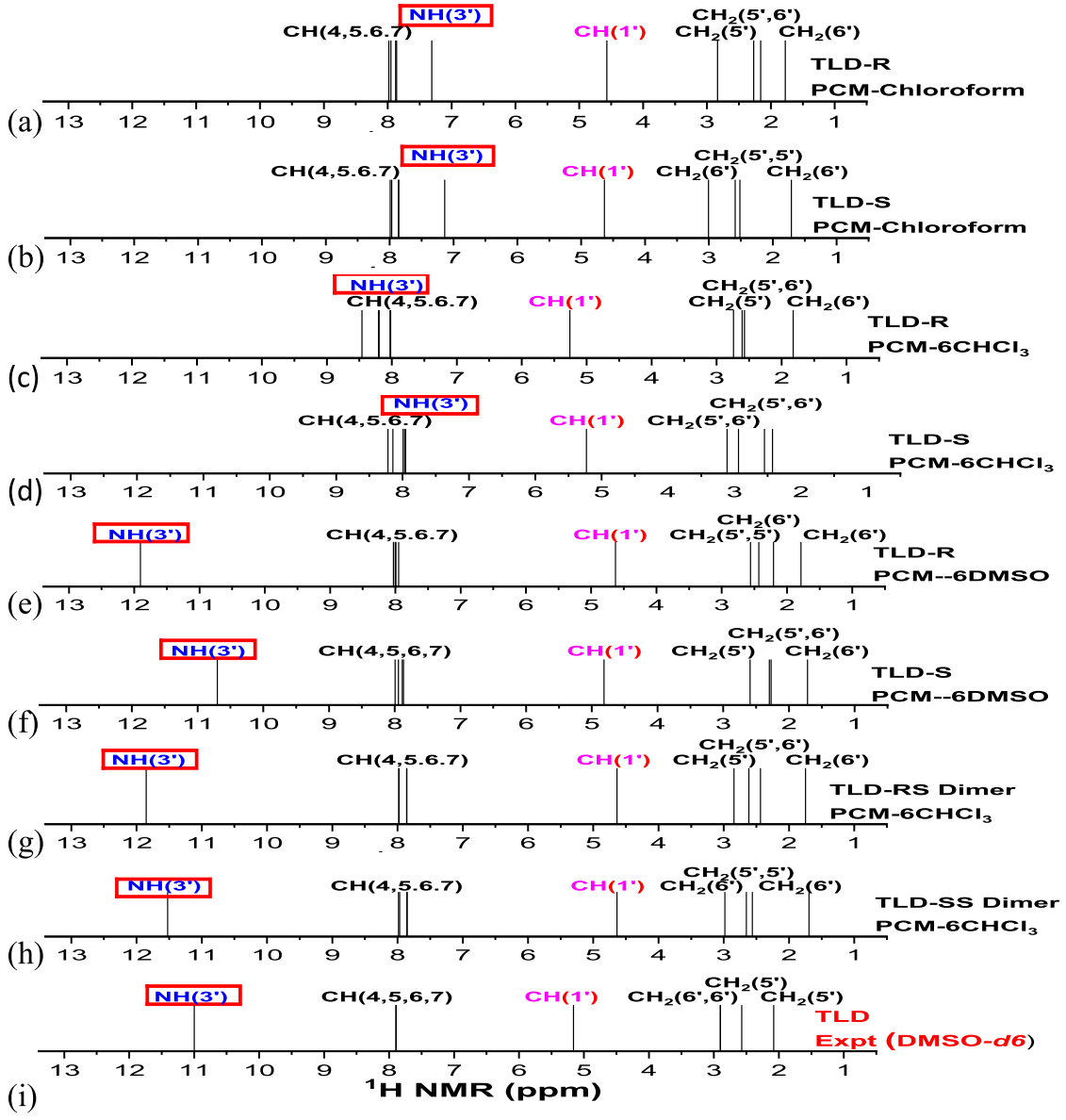

Figure 8. (a–h) B3LYP/6-31G(d,p)-PCM-Chloroform ^{1}H NMR spectra for TLD R and S monomer structures and (i) experimental spectrum in DMSO-d_6.

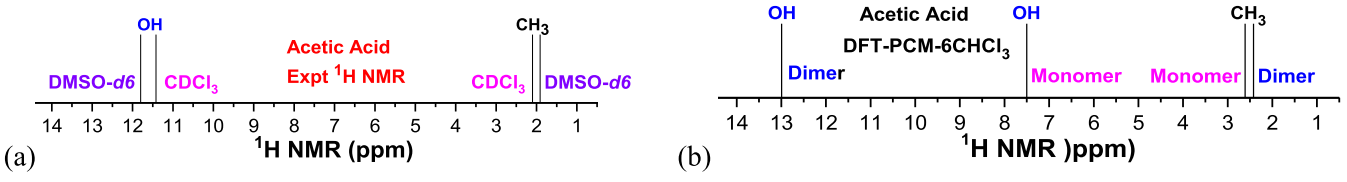

Figure 9. (a) Experimental ^{1}H NMR spectra ($CDCl_3$, DMSO-d_6) for acetic acid and (b) theoretical PCM-6$CHCl_3$ spectra.

basis set corresponds to approximately 15% of the energy of formation, which can be an estimate of the overestimation of complex energy due to the use of a small basis set (around approximately 3 kcal mol^{-1}). This would not invalidate our conclusion, since the energy of formation is much larger than this BSSE correction. The Pople's split-valence quality 6-311+G(2d,p) has a percentage BSSE correction of approximately 3% corresponding to a BSSE correction to the energy of formation of only 0.5 kcal mol^{-1}. The double-ζ Dunning basis set Aug-cc-pVDZ has a BSSE correction of 6% corresponding to a BSSE correction of 1.0 kcal mol^{-1} slightly higher than the 6-311+G(2d,p) basis set. As expected, the Aug-cc-pVTZ largest basis set has the smallest BSSE correction of 0.4 kcal mol^{-1} (2%). What we can conclude from Table 6 is that the energy of complex formation calculated with the small 6-31G(d,p) basis set, not corrected for BSSE, can provide a satisfactory description of the stability of the TLD-Guanine complex.

The energy of complex formation calculated including solvent effect with the PCM model (DMSO and water) drops to approximately −14 to −15 kcal mol^{-1} (ωB97x-D/6-31G(d,p)-

https://doi.org/10.1021/acsomega.3c05922
ACS Omega 2023, 8, 37521−37539

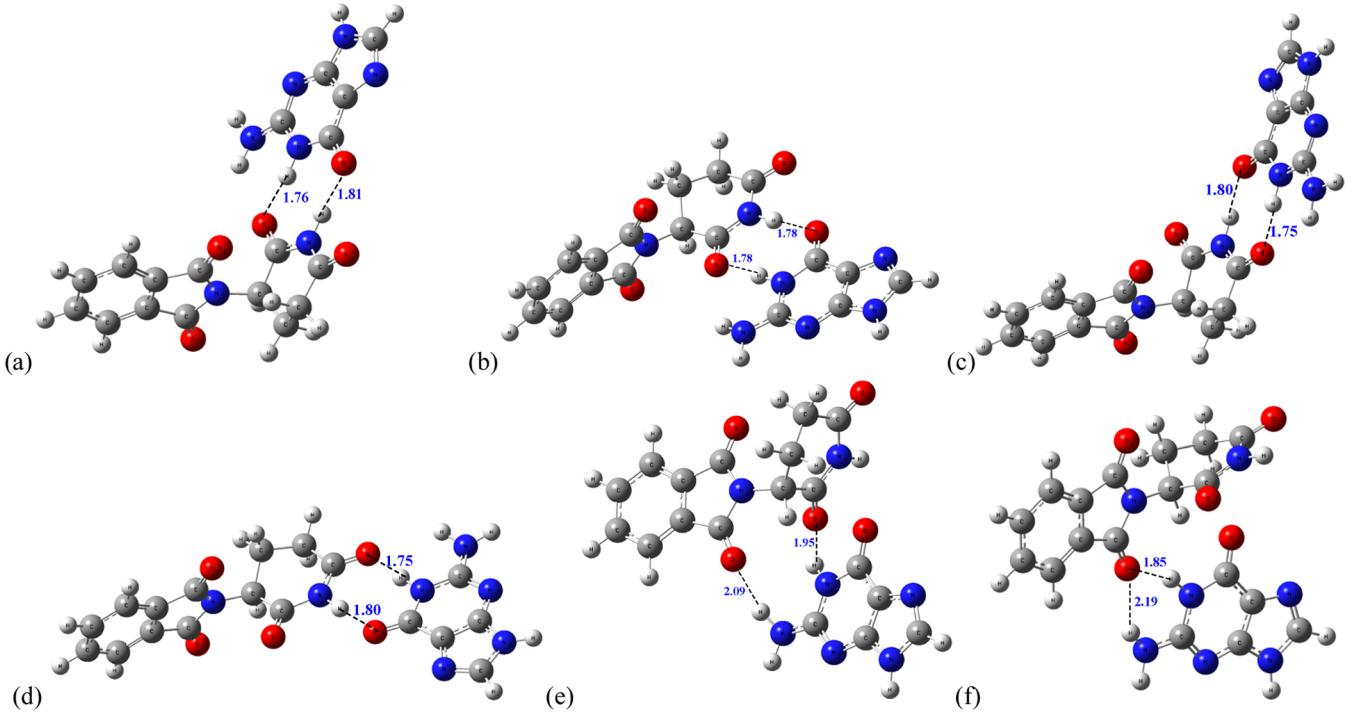

Figure 10. ωB97x-D/6-31G(d,p)-PCM-DMSO TLD-Monomer-Guanine complex optimized structures. (a) Gua-TLD-R-Monomer Complex-**I-R**, (b) Gua-TLD-S-Monomer Complex-**I-S**, (c) Gua-TLD-R-Monomer Complex-**II-R**, (d) Gua-TLD-S-Monomer Complex-**II-S**, (e) Gua-TLD-R-Monomer Complex-**III-R**, and (f) Gua-TLD-S-Monomer Complex-**III-S**.

PCM value), but it is still a sizable value conferring substantial stability to the complex formation in solution (see Table 7). The complexation process involving TLD molecular associations (dimer, trimer, and tetramer) was also considered. The energy of complex formation between guanine and the TLD multimer is in the range of approximately −11.0 to −13.0 kcal mol^{-1} very close to the free TLD complexes (involving the TLD monomer). This result leaves the possibility of the interaction of guanine with TLD associations very attractive, once the formation of TLD dimers was found to be very plausive according to the analysis of ^{1}H NMR data of TLD monomer. The strong H-bonds observed in the TLD-Guanine complexes are maintained when guanine interacts with TLD dimer, trimer, and tetramer, providing good stability for monomer and TLD associations complex with guanine. There are various possible dimeric, trimeric, and tetrameric TLD structures and we used the lowest energy ones to build the complex with guanine. Enthalpy and Gibbs free energies of formation are given in Table 7 in parentheses. While enthalpy and $\Delta E_{formation}$ resemble each other, $\Delta G_{formation}$ values are very small but still negative. Due to the high computational cost associated with DFT calculations on entire DNA structures, only the interaction with guanine was modeled. The presence of pentoses and phosphates can generate interesting effects, but, due to the enormous computational work, we focused on the interaction with guanine.

It should be mentioned that while enthalpy and energy of formation reported in Table 2 (TLD dimer) and Table 7 (TLD-Guanine complex) are very similar and substantially negative, predicting a favorable process based on energetic terms, the calculated $\Delta G_{formation}$ values are considerably smaller, even slightly positive. This is a result of the entropic effect, which is negative when two reactant molecules produce a single product, a well-known fact, which is the case of the dimer and complex formation from two TLD monomers and TLD and guanine molecules, respectively. This situation was reported previously for the β-CD···Sertraline inclusion complex,[58,59] where the experimental $T\Delta S$ data for complex formation, obtained from calorimetry titration, is positive while the corresponding theoretical value (assuming the common reaction of complex formation: β-CD + Sertraline → β-CD···Sertraline) is negative. An agreement with experimental data was obtained by modifying the reaction of complex formation including hydrated β-CD. Our thermodynamic data given in Table S1 are in line with the results from refs 58,59.

It can be seen from Figures 10−12 that TLD associations offered plenty of opportunities for the interaction with guanine, probably making the binding more effective and opening the possibility of having a 1:2 TLD-GUA complex involving two guanine molecules, for example. Guanine has three distinct **N−H** groups that can make strong H-bonds with TLD associations at different positions. The ^{1}H NMR spectrum of the TLD-Guanine complex will certainly exhibit a large **N−H** signal for the guanine proton, which should be readily observed experimentally and can be used to characterize the complex formation. It can be seen from Table 7 that the **Cpx-II-R** and **Cpx-II-S** structures are the preferred modes of interaction. Among the modes of interaction between guanine and TLD dimer, trimer, and tetramer, **Cpx-V**, **Cpx-VIII**, and **Cpx-X** structures are respectively the lowest energy ones. There are other possible modes of interaction involving $(TLD)_3$ and $(TLD)_4$ but we believe that Complexes **VII**, **VIII**, **IX**, and **X** can be considered representative structures. Therefore, complexes **Cpx-II** (TLD-GUA), **Cpx-V** ($(TLD)_2$-GUA), **Cpx-VIII** ($(TLD)_3$-GUA), and **Cpx-X** ($(TLD)_4$-GUA) should be considered as reasonable modes of interaction between TLD and guanine in solution.

The formation of the 1:2 TLD-Dimer-GUA complex was investigated, which was predicted to be stable relative to the

https://doi.org/10.1021/acsomega.3c05922
ACS Omega 2023, 8, 37521−37539

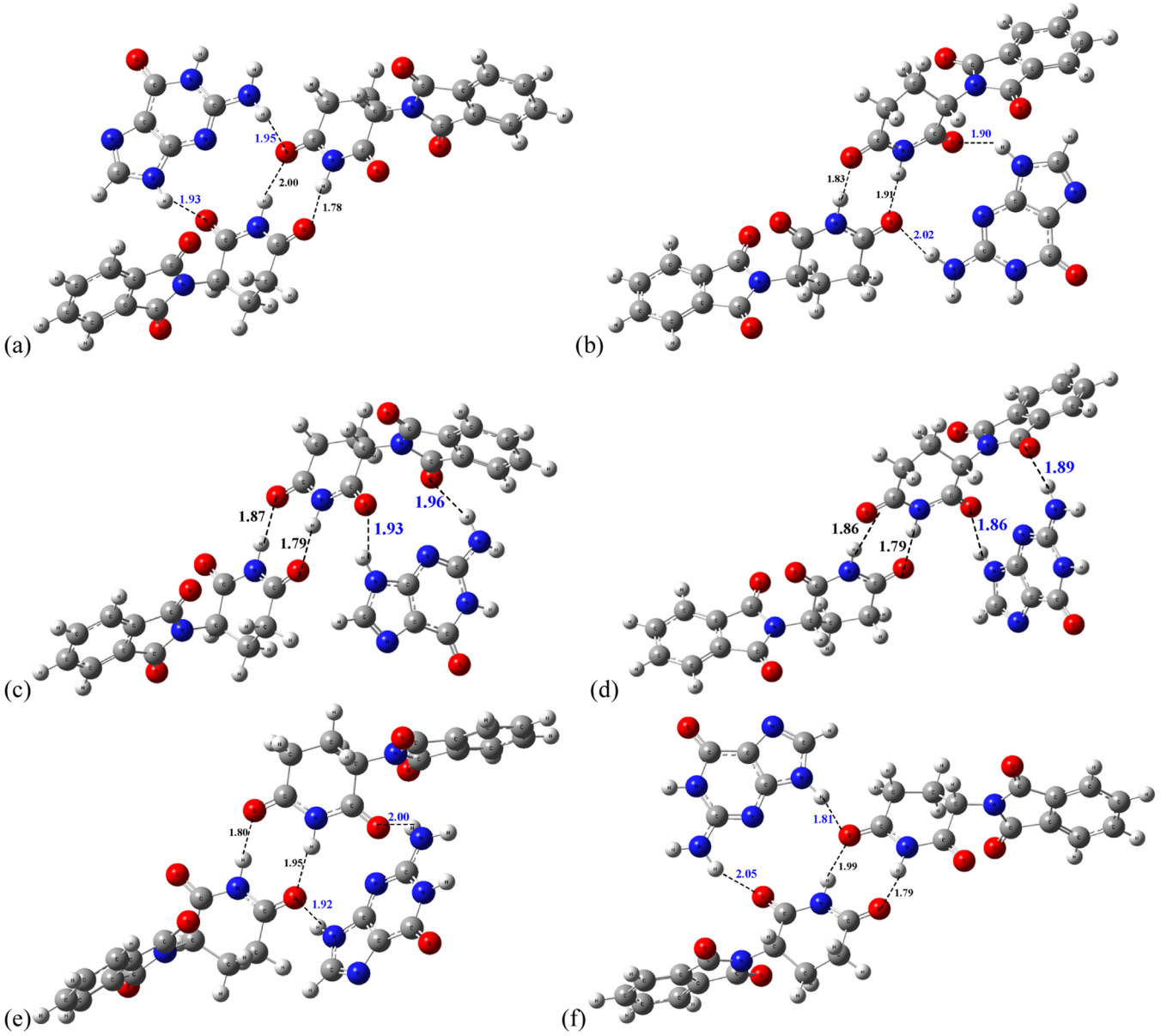

Figure 11. ωB97x-D/6-31G(d,p)-PCM-DMSO TLD-Dimer-Guanine complex optimized structures. (a) Gua-TLD-RS-Dimer Complex **IV**, (b) Gua-TLD-SS-Dimer Complex **IV**, (c) Gua-TLD-RS-Dimer Complex **V**, (d) Gua-TLD-SS-Dimer Complex **V**, (e) Gua-TLD-RS-Dimer Complex **VI**, and (f) Gua-TLD-SS-Dimer Complex **VI**.

TLD dimer and guanine. The same happened with 1:3 TLD-trimer-GUA and 1:4 TLD-tetramer-GUA complexes, indicating the plausibility of having intermolecular interactions involving various guanine molecules. DFT-PCM optimized 1:2, 1:3, and 1:4 complex structures are shown in Figures 13 and 14 along with TLD-Guanine N−H···O═C H-bond distances (Å). Relatively strong H-bonds are formed when more than one guanine unit interacts with TLD associations.

Calculated energies of complex formation and H-bond distances are listed in Table 8. The 1:4 TLD-tetramer-GUA complex is the strongest bound structure among all modes of TLD-Guanine interaction investigated. The results reported in Table 8 provide a strong indication of the existence of $(TLD)_n$-Guanine (n = 2, 3, 4) complexes having 1:2, 1:3, and 1:4 stoichiometry in solution, in addition to the TLD-Guanine complex. A crucial point to note is that the number of possibilities of interaction between TLD and guanine is high due to the presence of four N−H (guanine) and C═O (TLD) groups, enabling the formation of several distinct H-bonds. For stoichiometries different from 1:1 involving $(TLD)_n$, the number of possible H-bonds increases considerably, conferring more stability to the complexes. If the experimental ^{1}H NMR spectrum for the TLD-Guanine complex in DMSO-d_6 or $CDCl_3$ solution could be made available, then it would be possible to confirm the complex stoichiometry through a comparison of theoretical and experimental NMR spectra.

CONCLUSIONS

In addition to being previously known to cause teratogenicity, TLD and its derivatives have been found to be useful in anticancer drug research. The interaction with DNA bases has been experimentally verified, and a detailed investigation of the TLD-DNA complexation process is warranted. In this work, the molecular structure of TLD and its associations (dimer, trimer,

https://doi.org/10.1021/acsomega.3c05922
ACS Omega 2023, 8, 37521−37539

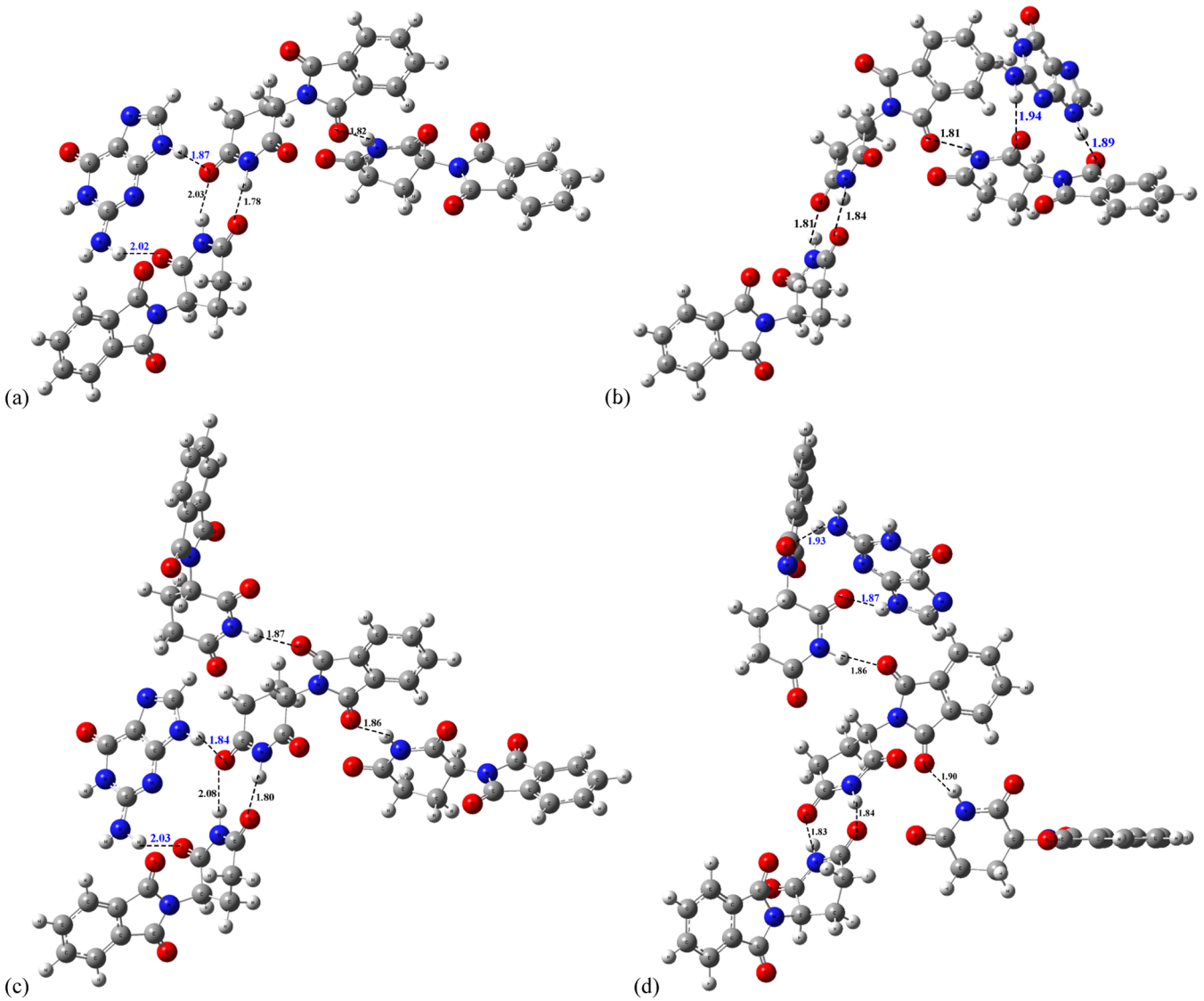

Figure 12. ωB97x-D/6-31G(d,p)-PCM-DMSO TLD-Guanine trimer and tetramer complex optimized structures. (a) Gua-TLD-**RS**-S Trimer Complex **VII**, (b) Gua-TLD-**RS**-S Trimer Complex **VIII**, (c) Gua-TLD-**RS**-**SS** Tetramer Complex **IX**, and (d) Gua-TLD-**RS**-**SS** Tetramer Complex **X**.

and tetramer) were investigated in DMSO and water solution using DFT methodology (ωB97X-D/6-31G(d,p)-PCM). Experimental ^{1}H NMR spectrum (in DMSO-d_6) was used as a reference for the determination of the preferred molecular structure present in DMSO solution. The formation of complexes between TLD and DNA basis guanine (GUA) in solution was investigated with various complex stoichiometries being considered, namely, TLD-GUA, $(TLD)_2$-GUA, $(TLD)_3$-GUA, $(TLD)_4$-GUA, $(TLD)_2$-2GUA, $(TLD)_3$-3GUA, and $(TLD)_4$-4GUA.

The initial purpose of this work was to assess if R/S enantiomers of TLD could be differentiated through thermodynamic or spectroscopic analysis in solution since one of the R/S forms is believed to be responsible for the teratogenic action of the TLD racemic mixture. DFT-PCM-DMSO calculations of relative energies and ^{1}H NMR chemical shifts were performed for R/S TLD structures using an implicit solvation model (PCM) and including a number (n) of explicit DMSO solvent molecules (n = 1, 2, 3, 4, 6, 8, 20). Our results show that both R/S forms of TLD are equally probable to be found in solution with maximum energy differences around ±2 kcal mol^{-1} being observed and very similar ^{1}H NMR spectrum. The experimental spectrum exhibited a remarkably large value of the **N**−**H** chemical shifts around 11 ppm, which could not be reproduced by the use of the PCM model. Only when explicit DMSO solvent molecules are included in the geometry optimization procedure, a full agreement with the experimental spectrum is obtained.

Next, the formation of TLD associations (dimer, trimer, and tetramer) was initially examined using all monomer combinations for a dimer (**RS**, **SS**, and **RR**). As the **RS** dimer was observed in the solid state, we extensively investigated the possibility of dimer structures surviving in solution (using the lowest energy **RS** dimer spatial orientation in further geometry optimization procedures for **SS** and **RR** dimers). All dimers have substantial negative values of the energy of formation. Subsequently, trimer and tetramer TLD structures were optimized using the DFT-PCM-DMSO methodology by combining TLD monomer (**R** and **S**) and dimer (**RR**, **RS**, and

https://doi.org/10.1021/acsomega.3c05922
ACS Omega 2023, 8, 37521−37539

Table 7. ωB97x-D/6-31G(d,p)-PCM Energy of Formation (in Units of kcal mol^{-1}) for TLD-Guanine Complexes

	$\Delta E_{formation}$ [a]					
TLD monomer	R	S	R	S	R	S
TLD-Guanine complex	Cpx-I		Cpx-II		Cpx-III	
PCM-DMSO-OPT-geometry	−13.9	−13.5	−14.5 (−11.7)[b] (−0.8)	−14.4 (−11.8)[b] (−0.6)[c]	−10.2	−11.7
PCM-water-OPT-geometry	−14.3	−13.9	−14.9	−14.8	−10.6	−12.1
TLD dimer	**RS**	**SS**	**RS**	**SS**	**RS**	**SS**
TLD-dimer-Gua complex	Cpx-IV		Cpx-V		Cpx-VI	
PCM-DMSO-OPT-geometry	−6.3	−7.7	−11.3	−8.1	−6.1	−5.4
PCM-water-OPT-geometry	−7.0	−8.6	−11.9	−13.2	−7.3	−6.5
TLD trimer	**RS**-S	**RS**-S				
TLD-trimer-Gua complex	Cpx-VII	Cpx-VIII				
PCM-DMSO-OPT-geometry	−6.8	−11.2				
PCM-water-OPT-geometry	−6.5	−11.1				
TLD tetramer	**RS-SS**	**RS-SS**				
TLD-tetramer-Gua complex	Cpx-IX	Cpx-X				
PCM-DMSO-OPT-geometry	−9.9	−14.5				
PCM-water-OPT-geometry	−5.8	−11.8				

[a]Energy of formation is defined as the difference between the total energy of the GUA-TLD complex and the sum of total energies of guanine and TLD monomer, dimer, trimer, and tetramer. [b]$\Delta H_{formation}$ are given in parentheses. [c]$\Delta G_{formation}$ are given in parentheses.

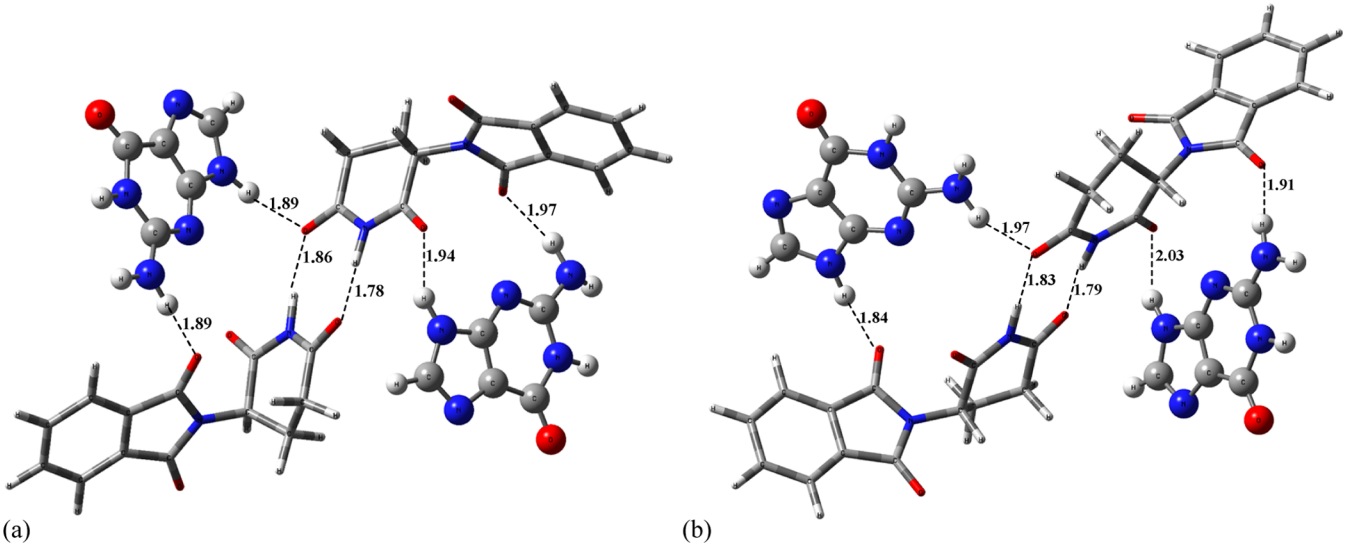

Figure 13. ωB97x-D/6-31G(d,p)-PCM-DMSO optimized complex structures formed between the TLD dimer and two guanine molecules: (a) TLD-**RS**-Dimer-2Guanine (Complex **XI**) and (b) TLD-**SS**-Dimer-2Guanine (Complex **XII**).

SS) structures. The resulting energy of formation values were found to be even more negative than those for dimers.

One interesting point is that the calculated ^{1}H NMR spectrum of dimers, trimers, and tetramers using the PCM model only (without explicit DMSO solvent molecules) is in fine agreement with the experiment profile with the **N−H** signal being correctly reproduced. These results provide strong support for the existence of TLD associations in the DMSO solution. When we changed to chloroform solvent, we found that the use of explicit $CHCl_3$ solvent molecules does not yield an agreement with experimental **N−H** ^{1}H NMR chemical shift values, as happened with the DMSO solvent. However, the TLD-**RS**-Dimer and TLD-**SS**-Dimer structures, with six explicit $CHCl_3$ solvent molecules included, show nice agreement with the experimental spectrum, strongly suggesting that the TLD dimer formation is responsible for the large **N−H** experimental chemical shift value.

To provide support to our proposal, we investigated the acetic acid monomer and dimer forms and compare the calculated and experimental ^{1}H NMR spectra in DMSO-d_6 and $CDCl_3$. The large OH ^{1}H NMR chemical shift value of 11.42 ppm in $CDCl_3$ (and 11.8 ppm in DMSO-d_6) can be reproduced only by the dimer structures in the case of chloroform solvent. The use of explicit $CHCl_3$ solvent molecules does not bring agreement with the experimental pattern. Our confirmation of the existence of the acetic acid dimer agrees with previous experimental studies. We then concluded that indeed the TLD is very likely to exist in solution as a molecular association (dimer, trimer, and tetramer).

Lastly, we investigated the formation of the 1:1 TLD-Guanine complex in solution, where three representative modes of interaction between TLD R/S and guanine were considered. Single-point energy calculations with improved basis sets (6-311+G(2d,p), aug-cc-pVDZ, and aug-cc-pVTZ) were carried out, and BSSE was calculated, validating our predicted energy of complex formation results. The energy of formation of the interaction of guanine with TLD associations is substantial, with strong N−H···O═C H-Bond formed. Other TLD-GUA complex stoichiometries were considered, 1:2, 1:3, and 1:4,

https://doi.org/10.1021/acsomega.3c05922
ACS Omega 2023, 8, 37521−37539

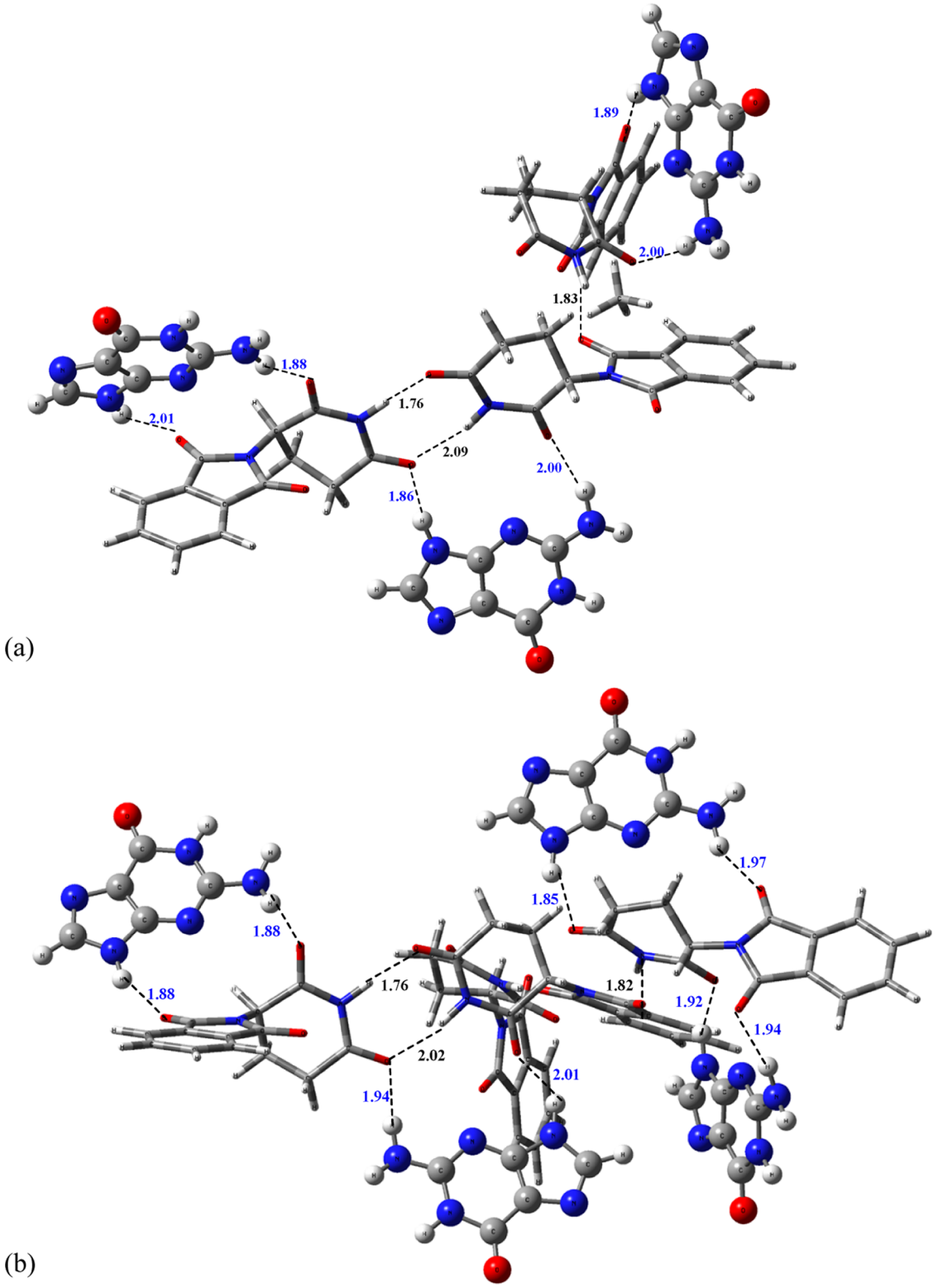

Figure 14. *ω*B97x-D/6-31G(d,p)-PCM-DMSO optimized complex structures formed between the TLD trimer and tetramer with three and four guanine molecules, respectively: (a) TLD-**RS**-S Trimer-3Guanine (Complex **XIII**) and (b) TLD-**RS**-SS-Tetramer-4Guanine (Complex **IV**).

involving TLD dimer, trimer, and tetramer. We found that these structures have a better energy of formation than the 1:1 complex and should be relatively stable in solution. TLD and guanine both have various N−H and C═O groups, respectively, that can act as H-bond donors and acceptors, making possible the existence of molecular associations in solution, instead of only one single TLD-GUA pair interacting. Our results provide new insight into the interaction of TLD with the molecular species in solution. According to our results, we must consider the plausibility of the existence of TLD associations (dimer, trimer, and tetramer) in solution when modeling the complexation of TLD with biological targets.

https://doi.org/10.1021/acsomega.3c05922
ACS Omega 2023, 8, 37521−37539

Table 8. ωB97x-D/6-31G(d,p)-PCM Energy of Formation (in Units of kcal mol^{-1}) for TLD-Dimer-Guanine 1:2, TLD-Trimer-Guanine 1:3, and TLD-Tetramer-Guanine 1:4 Complexes

	$\Delta E_{formation}$ (kcal mol^{-1})[a]		average N−H···O═C H-bond distance (Å)[b]			
TLD-dimer-2Gua	RS-2GUA: Cpx-XI	SS-2GUA: Cpx-XII	RS-2GUA: Cpx-XI		SS-2GUA: Cpx-XII	
			dimer	Dim-2GUA	dimer	Dim-2GUA
PCM-DMSO-OPT-Geom.	−18.6 (−11.3)[c]	−20.2 (−8.1)[c]	1.82 (1.83)[c]	1.92 (1.95)[c]	1.81 (1.83)[c]	1.94 (1.88)[c]
PCM-Water-OPT-Geom.	−19.9 (−11.9)[c]	−22.0 (−13.2)[c]				
TLD-trimer-3Gua	RS-S-3GUA: Cpx-XIII		RS-S-3GUA: Cpx-XIII			
			trimer	Tri-3GUA		
PCM-DMSO-OPT-Geom.	−28.0 (−11.2)[d]		1.89 (1.82)[d]	1.94 (1.92)[d]		
PCM-Water-OPT-Geom.	−30.3 (−11.1)[d]					
TLD-tetramer-4Gua	RS-SS-4GUA: Cpx-XIV		RS-SS-4GUA: Cpx-XIV			
			tetramer	Tet-4GUA		
PCM-DMSO-OPT-Geom.	−44.5 (−14.5)[e]		1.88 (1.86)[e]	1.93 (1.90)[e]		
PCM-Water-OPT-Geom.	−42.7 (−11.8)[e]					

[a]Energy of formation is defined as the difference between the total energy of GUA-TLD complex and the sum of total energies of guanine and TLD monomer, dimer, trimer, and tetramer. [b]Average value of all N−H···O═C H-bonds between TLD associations (dimer, trimer, tetramer) and TLD-Guanine subunits (Dimer-2Guanine, Trimer-3-Guanine, and Dimer-4-Guanine). [c]Data for the TLD-dimer-Guanine complex. [d]Data for the TLD-Trimer-Guanine complex. [e]Data for the TLD-Tetramer-Guanine complex.

■ ASSOCIATED CONTENT

Supporting Information

The Supporting Information is available free of charge at https://pubs.acs.org/doi/10.1021/acsomega.3c05922.

Additional figures and tables as well as the Experimental Section and optimized Cartesian coordinates of all structures (PDF)

■ AUTHOR INFORMATION

Corresponding Author

Wagner B. De Almeida − *Laboratório de Química Computacional e Modelagem Molecular (LQC-MM), Departamento de Química Inorgânica, Instituto de Química, Universidade Federal Fluminense (UFF), Niterói 24020-141 RJ, Brazil;* orcid.org/0000-0003-0785-2284; Email: wbdealmeida@gmail.com

Authors

Haroldo C. Da Silva − *Laboratório de Química Computacional e Modelagem Molecular (LQC-MM), Departamento de Química Inorgânica, Instituto de Química, Universidade Federal Fluminense (UFF), Niterói 24020-141 RJ, Brazil*

Isabel S. Hernandes − *Laboratório de Química Computacional e Modelagem Molecular (LQC-MM), Departamento de Química Inorgânica, Instituto de Química, Universidade Federal Fluminense (UFF), Niterói 24020-141 RJ, Brazil*

Complete contact information is available at: https://pubs.acs.org/10.1021/acsomega.3c05922

Notes

The authors declare no competing financial interest.

■ ACKNOWLEDGMENTS

W.B.D.A. thanks the Conselho Nacional de Desenvolvimento Científico e Tecnológico (CNPq) for a research fellowship (Proc. No. 309269/2021-0) and Fundação Carlos Chagas Filho de Amparo à Pesquisa do Estado do Rio de Janeiro (FAPERJ) for support (Proc. No. E-26/201.163/2021). H.C.D.S. thanks CNPq for a Ph.D. scholarship.

■ REFERENCES

(1) Elder, F. C. T.; Feil, E. J.; Snape, N.; Gaze, W. H.; Kasprzyk-Hordern, B. A. The Role of Stereochemistry of Antibiotic Agents in the Development of Antibiotic Resistance in the Environment. *Environ. Int.* **2020**, *139*, No. 105681.

(2) Brocks, D. R. Drug Disposition in Three Dimensions: An Update on Stereoselectivity in Pharmacokinetics. *Biopharm. Drug Dispos.* **2006**, *27* (8), 387−406.

(3) Kishimoto, T.; Yoshikawa, Y.; Yoshikawa, K.; Komeda, S. Different Effects of Cisplatin and Transplatin on the Higher-Order Structure of DNA and Gene Expression. *Int. J. Mol. Sci.* **2020**, *21* (1), 34.

(4) Kasprzyk-Hordern, B. Pharmacologically Active Compounds in the Environment and Their Chirality. *Chem. Soc. Rev.* **2010**, *39* (11), 4466.

(5) Smith, R. L.; Mitchell, S. C. Thalidomide-Type Teratogenicity: Structure activity Relationships for Congeners. *Toxicol Res.* **2018**, *7* (6), 1036−1047.

(6) Hague, D. E.; Idle, J. R.; Mitchell, S. C.; Smith, R. L. Racemates Revisited: Heterochiral Assemblies and the Example Ofscpdl/Scp-Thalidomide. *Xenobiotica* **2011**, *41* (10), 837−843.

(7) McBride, W. G. Thalidomide and Congenital Malformations. *Lancet* **1961**, *279*, 307 DOI: 10.1016/s0140-6736(62)91251-5.

(8) Burley, D. M.; Lenz, W. Thalidomide And Congenital Abnormalities. *Lancet* **1962**, *279*, 271 DOI: 10.1016/S0140-6736(62)91217-5.

(9) McBride, W. G. Thalidomide Embryopathy. *Teratology* **1977**, *16* (1), 79−82.

(10) Lenz, W. A Short History of Thalidomide Embryopathy. *Teratology* **1988**, *38* (3), 203−215.

(11) Bartlett, J. B.; Dredge, K.; Dalgleish, A. G. The Evolution of Thalidomide and Its IMiD Derivatives as Anticancer Agents. *Nat. Rev. Cancer* **2004**, *4* (4), 314−322.

(12) Łączkowski, K. Z.; Baranowska-Łaczkowska, A. Recent Studies on the Thalidomide and Its Derivatives. *Future Med. Chem.* **2018**, *10* (18), 2133−2136.

(13) Ito, T.; Ando, H.; Suzuki, T.; Ogura, T.; Hotta, K.; Imamura, Y.; Yamaguchi, Y.; Handa, H. Identification of a Primary Target of Thalidomide Teratogenicity. *Science* **2010**, *327* (5971), 1345−1350.

(14) Ito, T.; Handa, H. Another Action of a Thalidomide Derivative. *Nature* **2015**, *523* (7559), 167−168.

(15) Kim, H. K.; Seol, J. E.; Ahn, S. W.; Jeon, S.; Park, C.-S.; Han, J. Cereblon: Promise and Challenges for Combating Human Diseases. *Pflugers Arch. Eur. J. Physiol.* **2021**, *473* (11), 1695−1711.

(16) Asatsuma-Okumura, T.; Ito, T.; Handa, H. Molecular Mechanisms of the Teratogenic Effects of Thalidomide. *Pharmaceuticals* **2020**, *13* (5), 95.

(17) Suzuki, T.; Tanaka, M.; Shiro, M.; Shibata, N.; Osaka, T.; Asahi, T. Evaluation of Stability Difference between Asymmetric Homochiral Dimer in (S)-Thalidomide Crystal and Symmetric Heterochiral Dimer in (RS)-Thalidomide Crystal. *Phase Transitions* **2010**, *83* (3), 223−234.
(18) Tokunaga, E.; Yamamoto, T.; Ito, E.; Shibata, N. Understanding the Thalidomide Chirality in Biological Processes by the Self-Disproportionation of Enantiomers. *Sci. Rep.* **2018**, *8* (1), No. 17131, DOI: 10.1038/s41598-018-35457-6.
(19) Furberg, S.; Lemmich, J.; Cederberg, G.; et al. Structural Relationship between Thalidomide and Nucleosides. *Acta Chem. Scand.* **1965**, *19* (5), 1266 DOI: 10.3891/acta.chem.scand.19-1266.
(20) Petersen, C. S.; Leden, I.; Lindberg, B.; Holme, T.; Lindberg, A. A.; Craig, J. C. The Crystal Structure of N-(Alpha-Glutarimido)-4-Bromophthalimide. *Acta Chem. Scand.* **1969**, *23*, 2389 DOI: 10.3891/acta.chem.scand.23-2389.
(21) Oliveira, S. C. B.; Chiorcea-Paquim, A. M.; Ribeiro, S. M.; Melo, A. T. P.; Vivan, M.; Oliveira-Brett, A. M. In Situ Electrochemical and AFM Study of ThalidomideDNA Interaction. *Bioelectrochemistry* **2009**, *76* (1−2), 201−207.
(22) Baranowska-Łączkowska, A.; Banaszak-Piechowska, A.; Donarska, B.; Łaczkowski, K. Z. Towards Understanding the Interaction of (S)-Thalidomide with Nucleobases. *Arch. Biochem. Biophys.* **2020**, *693*, No. 108566.
(23) Parr, R. G.; Weitao, Y. *Density-Functional Theory of Atoms and Molecules*; Oxford University Press, 1995.
(24) Erkoç, Ş.; Erkoç, F. Quantum Chemical Investigation of Thalidomide Molecule. *J. Mol. Struct.: THEOCHEM* **2005**, *719* (1−3), 1−5.
(25) Lara-Ochoa, F.; Pérez, G. E.; Mijangos-Santiago, F. Calorimetric Determinations and Theoretical Calculations of Polymorphs of Thalidomide. *J. Mol. Struct.* **2007**, *840* (1−3), 97−106.
(26) Cipriani, P.; Smith, C. Y. Characterization of Thalidomide Using Raman Spectroscopy. *Spectrochim. Acta, Part A* **2008**, *69* (2), 333−337.
(27) Tian, C.; Xiu, P.; Meng, Y.; Zhao, W.; Wang, Z.; Zhou, R. Enantiomerization Mechanism of Thalidomide and the Role of Water and Hydroxide Ions. *Chem. − Eur. J.* **2012**, *18* (45), 14305−14313.
(28) Sardella, R.; Camaioni, E.; Macchiarulo, A.; Gioiello, A.; Marinozzi, M.; Carotti, A. Computational Studies in Enantioselective Liquid Chromatography: Forty Years of Evolution in Docking- and Molecular Dynamics-Based Simulations. *TrAC, Trends Anal. Chem.* **2020**, *122*, No. 115703.
(29) Xiong, F.; Zhou, L.; Chen, L.; Cao, F.; Zhang, S.; Zuo, Z. Discovery of Novel Potential CRBN Modulators through Structure-Based Virtual Screening and Bioassay. *J. Mol. Graphics Modell.* **2022**, *117*, No. 108325.
(30) Izumi, H.; Futamura, S.; Tokita, N.; Hamada, Y. Fliplike Motion in the Thalidomide Dimer:0.167em Conformational Analysis of (IR/i)-Thalidomide Using Vibrational Circular Dichroism Spectroscopy. *J. Org. Chem.* **2007**, *72* (1), 277−279.
(31) Meyring, M.; Mühlbacher, J.; Messer, K.; Kastner-Pustet, N.; Bringmann, G.; Mannschreck, A.; Blaschke, G. In Vitro Biotransformation of (IR/i)i-/i and (IS/i)i-/IThalidomide:0.167em Application of Circular Dichroism Spectroscopy to the Stereochemical Characterization of the Hydroxylated Metabolites. *Anal. Chem.* **2002**, *74* (15), 3726−3735.
(32) Walz, S.; Weis, S.; Franz, M.; Rominger, F.; Trapp, O. Investigation of the Enantiomerization Barriers of the Phthalimidone Derivatives EM12 and Lenalidomide by Dynamic Electrokinetic Chromatography. *Electrophoresis* **2015**, *36* (5), 796−804.
(33) Keltoum, D.; Tchouar, N.; Harkati, D.; Belaidi, S.; Bentayeb, K.; Rouane, A. Molecular Modeling of Reactivity and Vibrational Spectrum Raman of Thalidomide Enantiomers R and S Using Density Functional Theory and Hartree-Fock Methods. *Quantum Mech.* **2017**, *9*, 1421.
(34) Blanco, S.; Macario, A.; López, J. C. The Structure of Isolated Thalidomide as Reference for Its Chirality-Dependent Biological Activity: A Laser-Ablation Rotational Study. *Phys. Chem. Chem. Phys.* **2021**, *23* (24), 13705−13713.
(35) Mennucci, B.; Cancès, E.; Tomasi, J. Evaluation of Solvent Effects in Isotropic and Anisotropic Dielectrics and in Ionic Solutions with a Unified Integral Equation Method:0.167em Theoretical Bases, Computational Implementation, and Numerical Applications. *J. Phys. Chem. B* **1997**, *101* (49), 10506−10517.
(36) Chai, J.-D.; Head-Gordon, M. Long-Range Corrected Hybrid Density Functionals with Damped Atomatom Dispersion Corrections. *Phys. Chem. Chem. Phys.* **2008**, *10* (44), 6615.
(37) Hehre, W. J. *Ab Initio Molecular Orbital Theory*; Wiley, 1986.
(38) Da Silva, H. C.; De Almeida, W. B. Theoretical Calculations of 1H NMR Chemical Shifts for Nitrogenated Compounds in Chloroform Solution. *Chem. Phys.* **2020**, *528*, No. 110479.
(39) Hernandes, I. S.; Da Silva, H. C.; Dos Santos, H. F.; De Almeida, W. B. Conformational Analysis of 5,4-Dihydroxy-7,5,3-Trimethoxyisoflavone in Solution Using Sup1/SupH NMR: A Density Functional Theory Approach. *J. Phys. Chem. A* **2020**, *124* (25), 5182−5193.
(40) Hernandes, I. S.; Da Silva, H. C.; Dos Santos, H. F.; De Almeida, W. B. Unveiling the Molecular Structure of Antimalarial Drugs Chloroquine and Hydroxychloroquine in Solution through Analysis of Sup1/SupH NMR Chemical Shifts. *J. Phys. Chem. B* **2021**, *125* (13), 3321−3342.
(41) Wolinski, K.; Hinton, J. F.; Pulay, P. Efficient Implementation of the Gauge-Independent Atomic Orbital Method for NMR Chemical Shift Calculations. *J. Am. Chem. Soc.* **1990**, *112* (23), 8251−8260.
(42) Becke, A. D. Density-Functional Thermochemistry. III. The Role of Exact Exchange. *J. Chem. Phys.* **1993**, *98* (7), 5648−5652.
(43) Lee, C.; Yang, W.; Parr, R. G. Development of the Colle-Salvetti Correlation-Energy Formula into a Functional of the Electron Density. *Phys. Rev. B* **1988**, *37* (2), 785−789.
(44) Frisch, M. J.; Trucks, G. W.; Schlegel, H. B.; Scuseria, G. E.; Robb, M. A.; Cheeseman, J. R.; Scalmani, G.; Barone, V.; Mennucci, B.; Petersson, G. A.; Nakatsuji, H.; Caricato, M.; Li, X.; Hratchian, H. P.; Izmaylov, A. F.; Bloino, J.; Zheng, G.; Sonnenberg, J. L.; Hada, M.; Ehara, M.; Toyota, K.; Fukuda, R.; Hasegawa, J.; Ishida, M.; Nakajima, T.; Honda, Y.; Kitao, O.; Nakai, H.; Vreven, T.; Montgomery, Jr., J. A.; Peralta, J. E.; Ogliaro, F.; Bearpark, M.; Heyd, J. J.; Brothers, E.; Kudin, K. N.; Staroverov, V. N.; Kobayashi, R.; Normand, J.; Raghavachari, K.; Rendell, A.; Burant, J. C.; Iyengar, S. S.; Tomasi, J.; Cossi, M.; Rega, N.; Millam, J. M.; Klene, M.; Knox, J. E.; Cross, J. B.; Bakken, V.; Adamo, C.; Jaramillo, J.; Gomperts, R.; Stratmann, R. E.; Yazyev, O.; Austin, A. J.; Cammi, R.; Pomelli, C.; Ochterski, J. W.; Martin, R. L.; Morokuma, K.; Zakrzewski, V. G.; Voth, G. A.; Salvador, P.; Dannenberg, J. J.; Dapprich, S.; Daniels, A. D.; Farkas, Ö.; Foresman, J. B.; Ortiz, J. V.; Cioslowski, J.; Fox, D. J. *Gaussian 09*, Revision D.01; Gaussian, Inc.: Wallingford, CT, 2009.
(45) Vu, B. D.; Ba, N. M. H.; Phan, D. C. Facile Synthesis of Thalidomide. *Org. Process Res. Dev.* **2019**, *23* (7), 1374−1377.
(46) Varala, R.; Adapa, S. R. A Practical and Efficient Synthesis of Thalidomide via Na/Liquid NHsub3/Sub Methodologysup1/Sup. *Org. Process Res. Dev.* **2005**, *9* (6), 853−856.
(47) Caira, M. R.; Botha, S. A.; Flanagan, D. R. Polymorphism of N-(2,6-Dioxo-3-Piperidyl)Pthalimide (Thalidomide): Structural Characterization of a Second Monoclinic Racemic Modification. *J. Chem. Crystallogr.* **1994**, *24* (1), 95−99.
(48) Boys, S. F.; Bernardi, F. The Calculation of Small Molecular Interactions by the Differences of Separate Total Energies. Some Procedures with Reduced Errors. *Mol. Phys.* **1970**, *19* (4), 553−566.
(49) van Duijneveldt, F. B.; van Duijneveldt-van de Rijdt, J. G. C. M.; van Lenthe, J. H. State of the Art in Counterpoise Theory. *Chem. Rev.* **1994**, *94* (7), 1873−1885.
(50) Resende, S. M.; Almeida, W. B. De.; van Duijneveldt-van de Rijdt, J. G. C. M.; van Duijneveldt, F. B. A Converged Calculation of the Energy Barrier to Internal Rotation in the Ethylenesulfur Dioxide Dimer. *J. Chem. Phys.* **2001**, *115* (6), 2476−2482.
(51) Spectral Database for Organic Compounds (SDBS); ^{1}H NMR spectrum; SDBS-NMR-HSP-02-015; SDBS No.: 306; RN 64-19-7. https://sdbs.db.aist.go.jp/sdbs/cgi-bin/landingpage?spcode=NMR-HSP-02-015 (accessed May 10, 2023).
(52) Babij, N. R.; McCusker, E. O.; Whiteker, G. T.; Canturk, B.; Choy, N.; Creemer, L. C.; De Amicis, C. V.; Hewlett, N. M.; Johnson, P. L.; Knobelsdorf, J. A.; Li, F.; Lorsbach, B. A.; Nugent, B. M.; Ryan, S. J.;

Smith, M. R.; Yang, Q. NMR Chemical Shifts of Trace Impurities: Industrially Preferred Solvents Used in Process and Green Chemistry. *Org. Process Res. Dev.* **2016**, *20* (3), 661−667.
(53) Takis, P. G.; Papavasileiou, K. D.; Peristeras, L. D.; Boulougouris, G. C.; Melissas, V. S.; Troganis, A. N. Unscrambling Micro-Solvation of COOH and NH Groups in Neat Dimethyl Sulfoxide: Insights from Sup1/SupH-NMR Spectroscopy and Computational Studies. *Phys. Chem. Chem. Phys.* **2017**, *19* (21), 13710−13722.
(54) Heisler, I. A.; Mazur, K.; Yamaguchi, S.; Tominaga, K.; Meech, S. R. Measuring Acetic Acid Dimer Modes by Ultrafast Time-Domain Raman Spectroscopy. *Phys. Chem. Chem. Phys.* **2011**, *13* (34), 15573.
(55) Hernández-Lima, J.; Ramírez-Gualito, K.; Quiroz-García, B.; Silva-Portillo, A. L.; Carrillo-Nava, E.; Cortés-Guzmán, F. How solvent determines the molecular reactive conformation and the selectivity: Solvation spheres and energy. *Front. Chem.* **2022**, *10*, No. 1012769, DOI: 10.3389/fchem.2022.1012769.
(56) McQuarrie, D. A. *Statistical Thermodynamics*; HarperCollins Publishers, 1973.
(57) Dunning, T. H., Jr. Gaussian Basis Sets for Use in Correlated Molecular Calculations. I. The Atoms Boron through Neon and Hydrogen. *J. Chem. Phys.* **1989**, *90* (2), 1007−1023, DOI: 10.1063/1.456153.
(58) Passos, J. J.; De Sousa, F. B.; Lula, I. S.; Barreto, E. A.; Lopes, J. F.; De Almeida, W. B.; Sinisterra, R. D. Multi-Equilibrium System Based on Sertraline and -Cyclodextrin Supramolecular Complex in Aqueous Solution. *Int. J. Pharm.* **2011**, *421* (1), 24−33.
(59) Lopes, J. F.; Nascimento, C. S.; Anconi, C. P. A.; Santos, H. F. D.; Almeida, W. B. D. Inclusion Complex Thermodynamics: The -Cyclodextrin and Sertraline Complex Example. *J. Mol. Graphics Modell.* **2015**, *62*, 11−17.

https://doi.org/10.1021/acsomega.3c05922
ACS Omega 2023, 8, 37521−37539